INFLUENCE OF BORON NITRIDE ADDITION ON THE PERFORMANCE OF
HIGH TEMPERATURE PEM FUEL CELL BASED ON POLYBENZIMIDAZOLE
MEMBRANE

THE GRADUATE SCHOOL OF NATURAL AND APPLIED SCIENCES
OF
ATILIM UNIVERSITY

DEDAR EMAD HUSSIN

A MASTER OF SCIENCE
THESIS
IN
THE DEPARTMENT OF CHEMICAL ENGINEERING

FEBRUARY 2021

INFLUENCE OF BORON NITRIDE ADDITION ON THE PERFORMANCE OF
HIGH TEMPERATURE PEM FUEL CELL BASED ON POLYBENZIMIDAZOLE
MEMBRANE

A THESIS SUBMITTED TO
THE GRADUATE SCHOOL OF NATURAL AND APPLIED SCIENCES
OF
ATILIM UNIVERSITY

BY

DEDAR EMAD HUSSIN

IN PARTIAL FULFILLMENT OF THE REQUIREMENTS
FOR
THE DEGREE OF MASTER OF SCIENCE
IN
THE DEPARTMENT OF CHEMICAL ENGINEERING

FEBRUARY 2021

Approval of the Graduate School of Natural and Applied Sciences, Atilim University

—————————————

Prof. Dr. Ali Kara
Director

I certify that this thesis satisfies all the requirements as a thesis for the degree of Master of Science in Chemical Engineering, Atilim University.

—————————————

Prof. Dr. Şeniz Özalp Yaman
Head of Department

This is to certify that we have read the thesis INFLUENCE OF BORON NITRIDE ADDITION ON THE PERFORMANCE OF HIGH TEMPERATURE PEM FUEL CELL BASED ON POLYBENZIMIDAZOLE MEMBRANE submitted by DEDAR EMAD HUSSIN and that in our opinion it is fully adequate, in scope and quality, as a thesis for the degree of Master of Science.

—————————————

Assoc. Prof. Dr. Yılser Devrim
Supervisor

Examining Committee Members:

Prof. Dr. Necati Özkan
Polymer Science Dept., Middle East Technical Uni.   —————————————

Assoc. Prof. Dr. Yılser Devrim
Energy Systems Engineering Dept., Atılım University   —————————————

Assist. Prof. Dr. Enver Güler
Chemical Engineering Dept., Atılım University   —————————————

Date: *01.02.2021*

I hereby declare that all information in this document has been obtained and presented in accordance with academic rules and ethical conduct. I also declare that, as required by these rules and conduct, I have fully cited and referenced all material and results that are not original to this work.

Name, Last Name: Dedar Emad Hussin

Signature:

ABSTRACT

INFLUENCE OF BORON NITRIDE ADDITION ON THE PERFORMANCE OF HIGH TEMPERATURE PEM FUEL CELL BASED ON POLYBENZIMIDAZOLE MEMBRANE

Dedar Emad Hussin

M.S., Department of Chemical Engineering

Supervisor: Assoc. Prof. Dr. Yılser Devrim

February 2021, 57 pages

With the growth of the world population in the last decades, the energy demand has also increased due to technological developments and requirements. In this context, Proton exchange membrane fuel cell (PEMFC) has been gaining attention as an alternative to produce renewable energy lately thanks to its high efficiency, low pollution, high power density, and quiet operation. However, there must exist a high level of CO tolerance to be able to commercialize this alternative along with the use of reformed gasses produced from short processes, namely natural gas and methane – in abundant use today. High-temperature proton exchange membrane fuel cell (HT-PEMFC) allows for smooth water management and increased carbon monoxide (CO) tolerance to over 100 ℃ of operating temperature.

Against this backdrop, the present thesis is an attempt to design novel Polybenzimidazole/Boron Nitride (PBI/BN) composite membranes for HT-PEMFC application. BN was preferred due to its acceptable thermal stability, low electrical conductivity and high plasticizer property. This filler is used as 2.5, 5, 7.5 and 10 wt. %. The composite membranes are tested using thermogravimetric analysis (TGA), Scanning Electron Microscopy (SEM), mechanical analyses, acid doping/leaching, and proton conductivity measurements. Accordingly, thermal gravimetric analysis confirm the thermal stability of the PBI composite membranes; whereas acid leaching proves that adding more inorganic BN particles reduces acid loss from the membrane signifi-

cantly. Proton conductivity measurements show that introducing BN in the polymer matrix increases such conductivity, up to 0.260 S/cm at 180°C for PBI/BN-2.5

The HT-PEMFC performance test for PBI-BN-2.5 membrane is carried out in comparison with the PBI membrane, with results revealing that the former achieves higher performance with a current density of 136 mA/cm^2 at 0.6 V and 132 mW/cm^2 maximum power density at 165 $^{\circ}$C. The high performance of this MEA can be attributed to elevated proton conductivity and the enhanced properties of the PBI-BN-2.5 membrane. Overall, the findings in the present thesis show the usability of PBI/BN composite membranes in HT-PEMFCs, and their applicability for commercial fuel cell production upon further improvements.

Keywords: Proton Exchange Membrane, Fuel Cell, Composite Membrane, Polybenzimidazole, PBI, Boron Nitride

ÖZ

POLİBENZİMİDAZOLE TEMELLİ YÜKSEK SICAKLIK PEM YAKIT HÜCRESİNİN PERFORMANSINA BOR NİTRİT İLAVESİNİN ETKİSİ

Dedar Emad Hussin

Yüksek Lisans, Kimya Mühendisliği

Tez Yöneticisi: Doç. Dr. Yılser Devrim

Şubat 2021, 57 sayfa

Son yıllarda nüfus artışıyla birlikte, teknolojilerin büyümesiyle enerji talebi de artmıştır. Proton değişim membranlı yakıt pilleri (PEMFC), yüksek verimliliği, düşük kirliliği, yüksek güç yoğunluğu ve sessiz çalışması nedeniyle son yıllarda tercih edilen yenilenebilir enerji teknolojisi olarak kabul edilmiştir. PEMFC'lerin ticarileştirilmesi ve günümüzde sıklıkla kullanılan doğal gaz ve metan gibi kısa süreçlerden üretilen ıslah edilmiş gazların kullanımı için PEMFC'nin yüksek CO toleranslarına sahip olmalıdır. Yüksek sıcaklık proton değişim membranlı yakıt pili (HT-PEMFC), kolay su yönetimi ve 100 °C çalışma sıcaklığının üzerinde karbon monoksit (CO) toleransı sağlar.
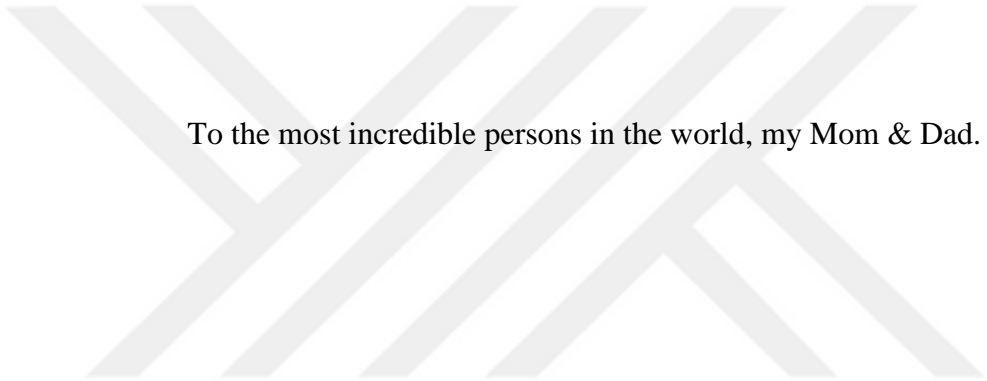
Bu tezde, HT-PEMFC uygulaması için yeni Polibenzimidazol/Bor Nitrür (PBI/BN) kompozit membranlar tasarlanmıştır. Yüksek termal kararlılık, düşük elektriksel iletkenlik ve yüksek plastikleştirici özelliği nedeniyle BN tercih edilmiştir. BN katkısı ağırlıkça 2.5, 5, 7.5 ve 10 % olarak kullanılmıştır. Kompozit membranlar, termogravimetrik analiz (TGA), Taramalı Elektron Mikroskobu (SEM) ve mekanik analizler, asit doping, asit sıyırılması, proton iletkenlik ölçümleri ile karakterize edildi. Termal gravimetrik analiz, PBI/BN kompozit membranların HT-PEMFC uygulaması için termal kararlılığını doğrulamıştır. Asit sıyırılması testi sonuçları, daha fazla inorganik BN parçacığı eklenmesinin membrandan asit kaybını önemli ölçüde

azalttığını göstermiştir. Proton iletkenlik ölçümleri, polimer matrisine BN eklenmesinin proton iletkenliğini artırdığını göstermiştir. En yüksek proton iletkenlik değeri 180°C'de 0,260 S/cm olarak PBI/BN-2.5 membranda elde edilmiştir.

PBI/BN-2.5 kompozit membranının HT-PEMFC performans testi, PBI membran ile karşılaştırılarak incelenmiştir. Test sonuçlarına göre 165 ^{o}C'de PBI-BN-2.5 membran, 0.6 V ve 132 mW/cm^2 maksimum güç yoğunluğunda 136 mA/cm^2 akım yoğunluğu ile PBI membrandan daha yüksek performansa sahiptir. Bu MEA'nın yüksek performansı, PBI-BN-2.5 membranının yüksek proton iletkenliğine ve gelişmiş özelliklerine bağlanabilir. Tez çalışmasında elde edilen sonuçlar PBI/BN kompozit membranların HT-PEMFC'lerde kullanılabilirliğini göstermiştir. Gelecekteki geliştirme çalışmaları ile PBI/BN membranlar ticari yakıt hücrelerinde de kullanılabilir.

Anahtar Kelimeler: Proton Değişim Membran, Yakıt Pili, Kompozit Membran, Polibenzimidazole, PBI, Bor Nitrür.

To the most incredible persons in the world, my Mom & Dad.

ACKNOWLEDGMENTS

I would like to express my sincere thanks and gratitude to my supervisor, Assoc. Prof. Dr. Yılser Devrim, for her guidance, criticism, encouragement, insight, due and invaluable advices, and patience throughout the research period – mostly for teaching me about fuel cells and giving me inspiration to work and experience in this field in the future.

I wish to thank my family for their exceptional support. I owe much to my parents, who love, care, continuously sacrifice, and encourage me at crucial moments. In addition, I would like to thank my grandparents, Makea & Ibrahim, my beloved sister, Deyarie, and brothers, Ahmed & Omer for their support. Moreover, many special thanks to my dear friends, Mustafa Y. Mohammed, Maha Jalal, Noor Ayad & Mais Al-bayati.

This work I dedicate to my late grandparents, Bahija & Hussin.

TABLE OF CONTENTS

LIST OF TABLES

TABLES

LIST OF FIGURES

LIST OF SYMBOLS/ABBREVIATIONS

AFC	Alkaline Fuel Cell
ADL	Acid Doping Level
AL	Acid Leaching
BN	Boron Nitride
B-PEI	Branched Polythyleneimine
$CaTiO_3$	Calcium Titanate
CL	Catalyst Layer
CO	Carbone Monoxide
CCM	Catalyst Coated membrane
DMFC	Direct Methanol Fuel Cells
DMAc	N,N-dimethylacetamide
Ea	Activation Energy
EIS	Electrochemical Impedance Spectroscopy
Fe_2TiO_5	Iron Titanium Oxide
GDE	Gas Diffusion Electrode
GDL	Gas Diffusion Layer
GO	Graphene Oxide
H	Hydrogen
H_2O	Water
HT-PEMFC	High temperature PEMFC
h-BN	Hexagonal Boron Nitride
H_3PO_4	Phosphoric Acid
KOH	Potassium Hydroxide
K_2CO_3	Potassium Carbonate
LT-PEMFC	Low temperature PEMFC
$LiALO_2$	Lithium Aluminum Carbonate
MCFC	Molten Carbonate Fuel Cells
MEA	Membrane Electrode Assembly
MWCNT	Multi walled carbon nanotubes

O_2	Oxygen
PAFC	Phosphoric Acid Fuel Cells
PAAM	Polyacrylamide
PEM	Polymer Electrolyte Membrane
PEMFC	Proton Exchange Membrane Fuel Cell
PFSA	Perflorosulfonic Acid
PPA	Polyphosphoric Acid
PTFE	Polytetrafluoroethylene
PBI	Polybenzimidazole
PC	Proton Conductivity
PT	Platinum
PVA	Polyvinyl
r	Resistance
SiO_2	Silicon dioxide
SOFC	Solid Oxide Fuel Cells
SEM	Scanning Electron Microscopy
Tg	Glass transition temperature
TGA	Thermo Gravimetric Analysis
TiO_2	Titanium dioxide
W	Width
W_{PA}	Weight of acid doped membrane
W_{dry}	Weight of dry membrane
ZrP	Zirconium Phosphide
ΔG	Change of Gibbs free energy
ΔH	Change in Enthalpy
ΔL	Change of Length
μCHP	Micro generation
Ŋtheo	Efficiency of Fuel Cell
L	Thickness of Membrane
lo	Original Length

CHAPTER 1

INTRODUCTION

With the growing world population and technology, the need for energy also keeps on increasing. Thus, low-cost and sustainable energy production and efficient renewable fuels are becoming ever more of a necessity. In this sense, the country's economic and social growth also relies on the related benefits [1]; henceforth, renewable energy projects are making major strides and fuel cells have become the tools that generate electrical energy with chemical energy without the need for burning fuel. Without combustion, the high energy losses and toxic emissions typically associated with the combustion process are eliminated from the cycle [2]. In detail, a fuel cell is an electrochemical device, which converts directly into electrical energy the chemical energy of a reaction between a fuel (on the anode side) and an oxidant (on the cathode side). It consists of one electrolyte and two electrodes, one positive and one negative. The fuel and oxidant are pumped into the fuel cell outside. On the anode side, the fuel is converted into its protons and electrons, and an external circuit carries the electrons to the cathode side, while the protons are carried through the electrolyte [3].

1.1 History

Initially, William Robert Grove came up with the first fuel cell principle and published his findings in 1839 [4]. His design was based on the principle of generating hydrogen (H_2) and oxygen (O_2) gases as an energy. Grove used the sulfuric acid electrolyte and a platinum electrode to create the first H_2- O_2 fuel cell. The design included the cells that produced hydrogen and oxygen gases to initiate electron transfer to the upper cell. Therefore, the energy produced from the bottom cell is used for the electrolysis of water and, in turn, releasing hydrogen and oxygen gases.

.
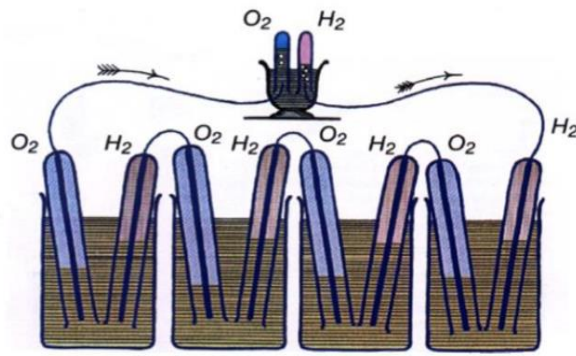
Figure 1.1 The first fuel cell, as introduced by William R. Grove.

Following this innovation, nearly a hundred researchers attempted to upgrade Grove's cell into a practical device. In the late 1930s, Francis Thomas Bacon began researching alkali electrolyte fuel cells (with potassium hydroxide); this was the first large-scale fuel cell stack up until the late 1950s. Bacon's fuel cells attracted the attention of Pratt & Whitney, who adopted his work to power the Apollo spacecraft. Thomas Grubb and Leonard Niedrach later came up with low-temperature proton exchange membrane fuel cell (PEMFC) technology developed at General Electric in 1955. This was the first fuel cell system to find its ways into real-life application, used as a power source for NASA space flights to Gemini in the 1960s [5]. The establishment of the California Fuel Cell Partnership to develop and sell zero-emission vehicles further stimulated PEMFC research. In the beginning, the cell was costly to build as the catalyst electrodes used Pt, whose loading would have been as high as 30 mg Pt/cm^2 [6]. In the early 1990s, the Pt load was significantly reduced to about 0.5 mg Pt/cm^2 by supporting the Pt particles on a graphic carbon board, thereby considerably improving the catalytic surface area and the subsequent output [7]. The layer of catalysts was bound directly to the membrane.

Combined with the rise in energy prices, this discovery led to active research and development on PEMFCs that continues today. Nowadays, fuel cells have far broader applications than any other currently available power sources. According to the American Energy department, fuel cells are the leading candidates for light-duty cars, houses, and possibly even smaller applications such as a replacement for rechargeable batteries. Therefore, it would be fair to state that fuel cells are likely to have a promising future.

2

In 1800 W. Nichols, A. Carlisle explains how water is electrolysed.

In 1838 First "carbon battery" is developed by Sir W. Grove.

In 1893 F.W. Ostwald describes the theoretical performance of fuel cells.

In1921 Experiment with solid oxide electrolyte at high temperatures.

In 1939 F.T Bacon starts research into alkaline fuel cells.

In1955 T. Grubb develops the sulphonated polystyrene ion exchange membrane.

In 1959 the Central Institute of Technology and GE begins research into solid oxide fuel cells.

Figure 1.2 Historical development of fuel cells [8].

1.2 Types of Fuel Cell

Figure 1.3 illustrates the fuel cells classified by electrolyte and working temperature.
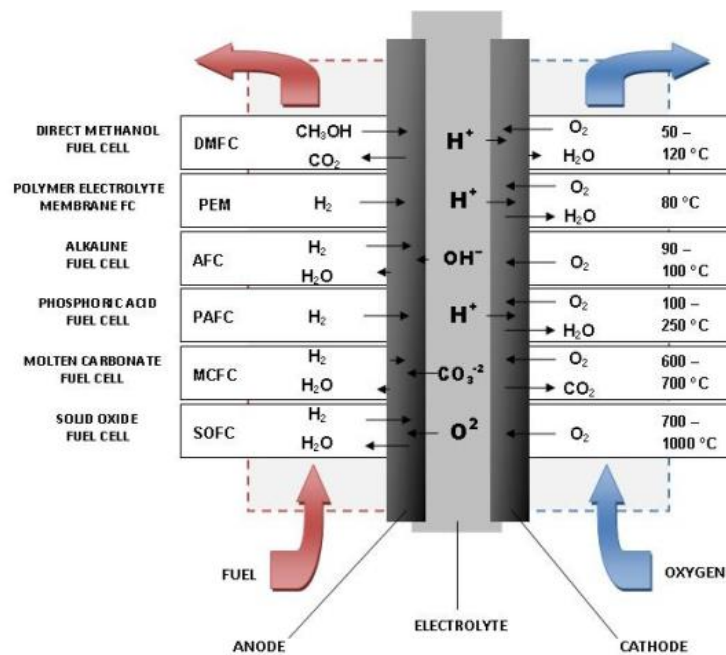
Figure 1.3 Different kinds of fuel cells with unique fuel intakes and electrochemical reactions [9].

3

1.2.1 Alkaline Fuel Cell (AFC)

AFC uses alkaline electrolyte potassium hydroxide (KOH) to produce electric energy in an aqueous solution. The presence of hydroxyl ions passing through the electrolyte generates a c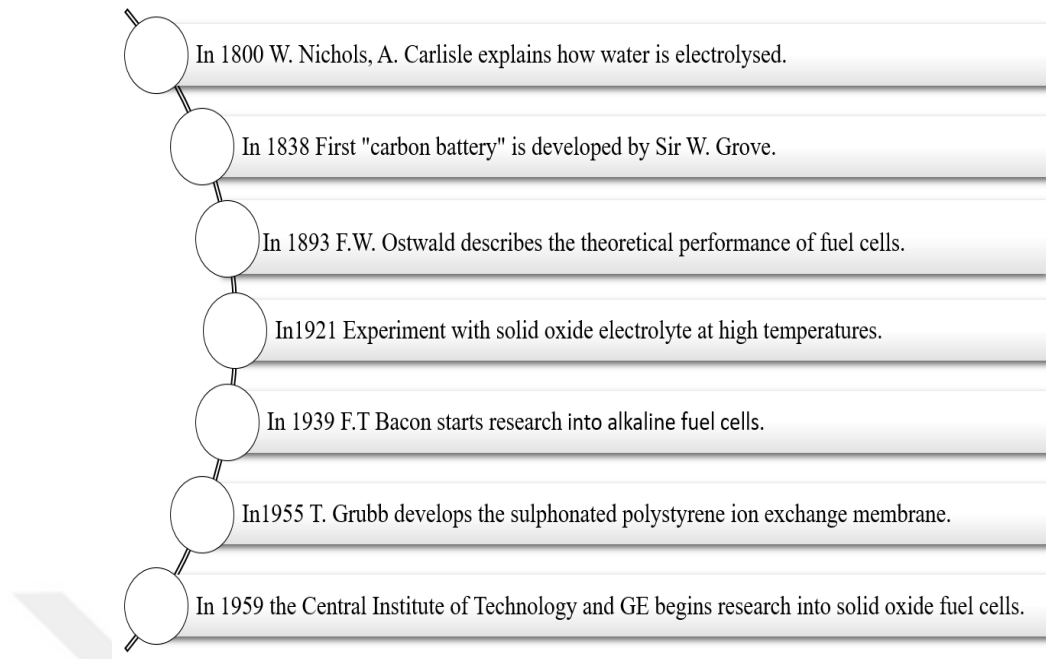hain, making it possible to receive electric energy. The AFCs operating temperature is greater than 60 °C, now capable of operating at even lower temperatures. The catalysts of a nickel speed up electrochemical reactions on the cathode and anode side. The electrical efficiency of AFCs is approximately 50%, and when the generated heat is consumed, this ratio exceeds 80% [10]. Due to its more comprehensive range of robust materials, lower-cost parts, low working temperature, and quick start-up, AFCs are favored in military, aerospace, reserve power, and transportation areas. Yet, they have some fuel and air drawbacks in terms of aqueous electrolyte handling and CO2 sensitivity

1.2.2 Phosphoric Acid Fuel Cell (PAFC)

PAFC was the first commercially available fuel cell in the market, consisting of a porous matrix surrounded by porous carbon electrodes, which hold the electrolyte liquid phosphoric acid. Apart from the nature of the electrolyte, the PAFC structure is similar to the Proton Exchange Membrane Fuel Cell (PEMFC) with porous carbon electrodes and carbon gas diffusion layer located on either side of the Membrane Electrode Assembly (MEA). Compared to PEMFC, the efficiencies are almost similar, but the power densities are lower. They are highly resistant to impurities from fuel, and their operating temperature is adequate to allow micro-generation (μCHP). Still, the operating temperature is not high enough to meet the precious metal catalyst requirements [11].

1.2.3 Molten Carbonate Fuel Cell (MCFC)

The MCFC electrolyte is a liquid mixture of alkali metal carbonates, lithium carbonate (Li_2CO_3), and potassium carbonate (K_2CO_3) retrained in a $LiAlO_2$ porous ceramic matrix. MCFC can be equipped with internal reforming process facilities that transform the hydrocarbon directly into H_2 inside the fuel cell by the nature of their high operating temperatures. MCFC systems can also use gaseous hydrocarbons such as methane, methanol, petroleum, or coal gas. The applied electrodes are Nick-

el-based and allow for catalytic activity and conductivity. The system can be used with turbine cycle µCHP and hybrid gas, with the main disadvantage being the use of a highly corrosive and molten electrolyte [12].

1.2.4   Solid Oxide Fuel Cell (SOFC)

Otherwise known as rigid fuel cells due to the presence of solid electrolytes, these cells can operate at high-temperatures. The electrolyte is made of zirconium Oxide (ZrO_2), or Zirconia. The first application was in the 1930s, and it remained so until the 1960s as a n average functioning and successful electrolyte. The reaction of SOFC consists of hydrogen and oxygen as fuel and water production. As mentioned before, it operates at high-temperatures, thus qualifying it for internal reforming and allowing for rapid electro-catalysis with metals that are non-precious to generate extremely high heat for µCHP. The efficiency can be maximized to 70 % with µCHP, and SOFC can be useful in industrial and power stations to generate high voltage [13].

1.2.5   Proton Exchange Membrane Fuel Cell (PEMFC)

The Proton Exchange Membrane (PEM) is one of the most preferred types of fuel cells nowadays. The principal component of a PEMFC is the membrane electrode unit (MEA) as a solid polymer electrolyte bonded to porous catalyzed electrodes (anode and cathode) located on either side. Both anode and cathode are normally composed of a conductive carbon catalyst comprising Pt. After improving the performance of PEMFC to more than 50 %, it started to gain more application as a primary energy source for different systems [14]. The materials used consist of a fluorocarbon polymer, like Teflon, bounded by sulfonic acid groups. Acid molecules bind to the polymer so as not to escape, which renders them the freedom to pass through the membrane. Electrolyte loss is no longer a concern with the application of solid-type polymer electrolytes [15]. PEMFCs are grouped as low temperature (LT-PEMFC) and high temperature (HT-PEMFC) according to the working environment, with the former operating between 60-80 °C, and the latter between 120-200 °C [16].

1.3   Operation of PEMFC

Figure 1.4 shows the working principle of the PEMFC. A membrane electrode assembly (MEA) is at the center to combine electrodes and electrolytes to produce electric power when supplied with reactant gases. Thin gaseous diffusion layers are coated with electro-catalysts on either side of the electrolyte membrane where electrochemical reactions occur [17]. Collector/separator plates are sandwiched between the MEA. In a multi-cell configuration, these collector plates attach the cathode of one cell both physically and electrically to the anode, hence the term "bipolar plates". Reactant gases flow through the bipolar plates flow fields as required. These fields have a drastic effect on PEMFC efficiency, which can have electrochemical reactions on both the anode and cathode sides of the cell. The main cell components of the PEMFC are shown in Figure 1.5.
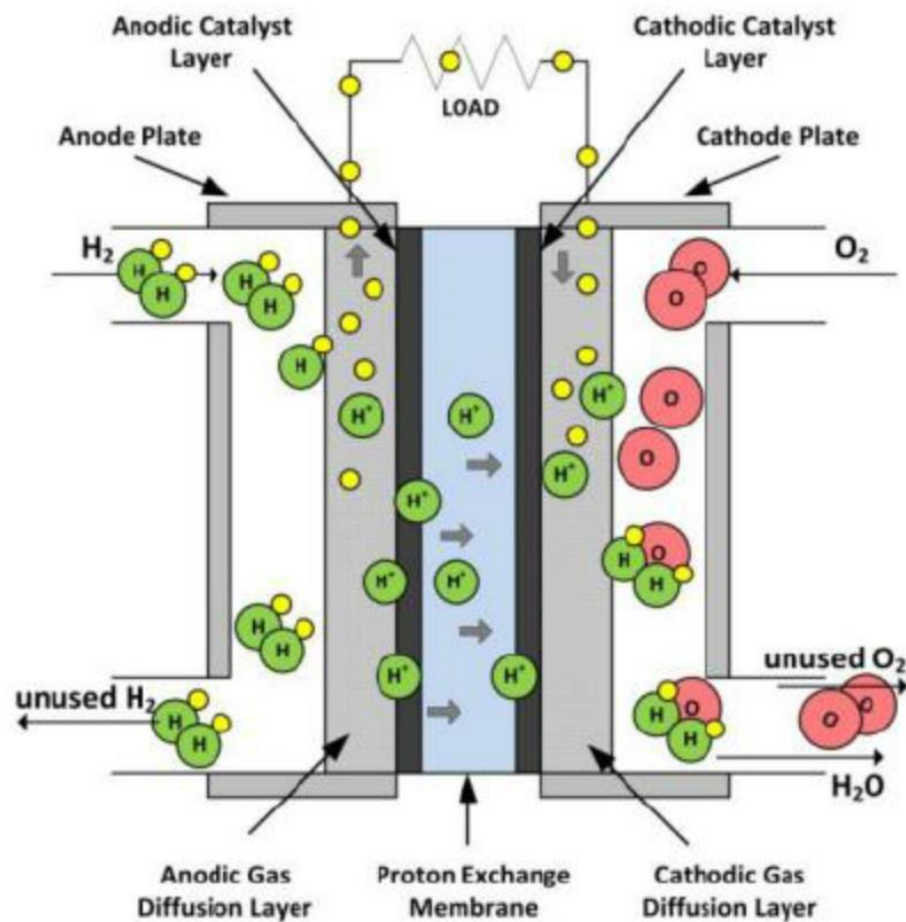
Figure 1.4 Operation of a single-cell of PEMFC.
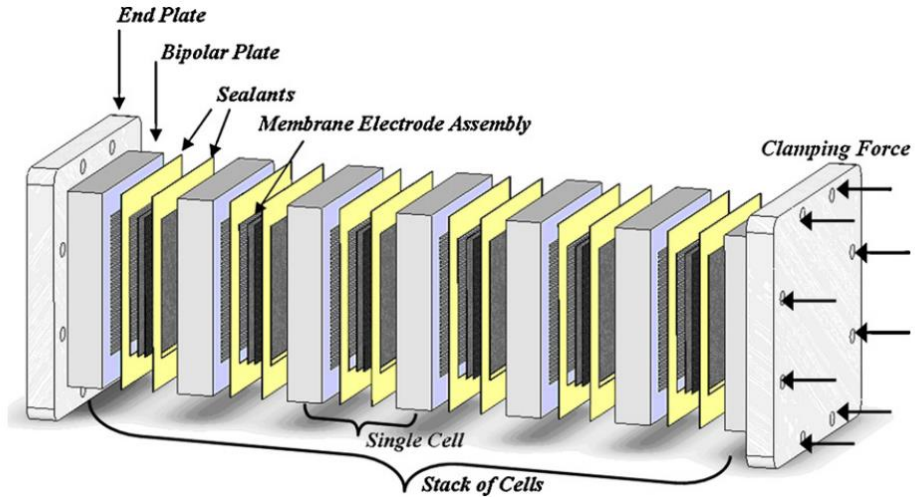
Figure 1.5 Schematic view of the PEMFC stack hardware hardware [18].

The following processes take place inside the PEMFC[19]:

- Reactant gases flow through the bipolar plates.
- At the anode side, H_2 diffuses the catalyst layer through the porous media.
- Electrochemical reactions take place and H_2 splits into protons and electrons.
- Protons transfer through proton conductive polymer electrolytes.
- The electrons are unable to pass through the conductive proton layers, and instead conduct with electrically conductive elements of the cells.
- At the cathode side, the O_2 protons and electrons from the external circuit are combined to produce water.
- Water droplets exit the cell due to excess reactive gases.

Fuel cell design should be optimized to obtain minimum obstruction during the operations. For this, all the components are selected according to the operation temperature and the corrosive nature of the chemicals. Understanding these processes and the importance of the components helps increase the fuel cell performance.

1.4 Thermodynamic and Kinetic for PEMFCs

A fuel cell reaction contains two half-cell electrochemical reactions that occur at anode and cathode sides. H_2 is oxidized to form two protons and two electrons at the anode side (Equation 1). The protons and electrons combine with oxygen to form water at the cathode side (Equation 2).

Anode reaction: $H_2 \rightarrow 2H^+ + 2e^-$ (1)

Cathode reaction: $\frac{1}{2} O_2 + 2H^+ + 2e^- \rightarrow H_2O$ (2)

Overall cell reaction: $H_2 + \frac{1}{2} O_2 \rightarrow H_2O$ (3)
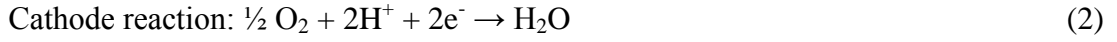
The total reaction enthalpy is determined as the change between the products heat-forming and the reactants heat-forming, as illustrated in Equation (4):

$$\Delta H = (hf)_{H_2O} - (hf)_{H_2} - \frac{1}{2}(hf)_{O_2}$$ (4)

The heat of water formation is equal to (-286 kJ/mol) at room temperature, whereas the heat of H_2 and O_2 is equal to zero. Each reaction involves entropy, and each charge must overcome the obstacle of the activation energy to produce energy through moving the PEMFC. The energy emitted is equal to the free energy shift in Gibbs between the products and the reactants [20], [21].

The potential of a fuel cell is (1.23 V), which can be calculated using Equation (5):

$$\Delta G = -nFE = \Delta H - T\Delta S$$
(5)

The ratio between the change of Gibbs free energy (ΔG) and the change of enthalpy (ΔH) in a reaction represents the maximum theoretical efficiency (η_{theo}) of a fuel cell. $\eta theo$ can be calculated from Equation (6):

$$\eta_{theo} = \frac{\Delta G}{\Delta H} = \frac{237}{286} \times 100 \cong 83\%$$
(6)

The calculation of the theoretical fuel cell potential of H_2/O_2 at 25 °C and 1 bar of pressure can be determined as in Equation (7):

$$E = \frac{-\Delta G}{nF} = \frac{237}{96485 \times 2} = 1.23\ V$$ (7)

The potential can be suitable to the gaseous water condition, which attains about 1.118 V as PBI-based PEMFCs operates at very high temperatures. The losses (ΔV_{loss}) caused by kinetics and dynamics of the procedures cause the actual potential

8

and the actual efficiency to fall short of the theoretical values. Equation (8) shows the actual fuel cell potential in terms of E (OCV) and ΔV_{loss}.

$$V_{cell} = E - \Delta V_{loss}$$
(8)

In terms of the losses, the cell voltage of PEMFC can be illustrated as in Equation (9):

$$V\_cell = E - (\Delta V_{actl} + \Delta V_{ohm} + \Delta V_{conc})$$
(9)

Figure 1.6 illustrates the voltage-current relationship and the anticipated losses.
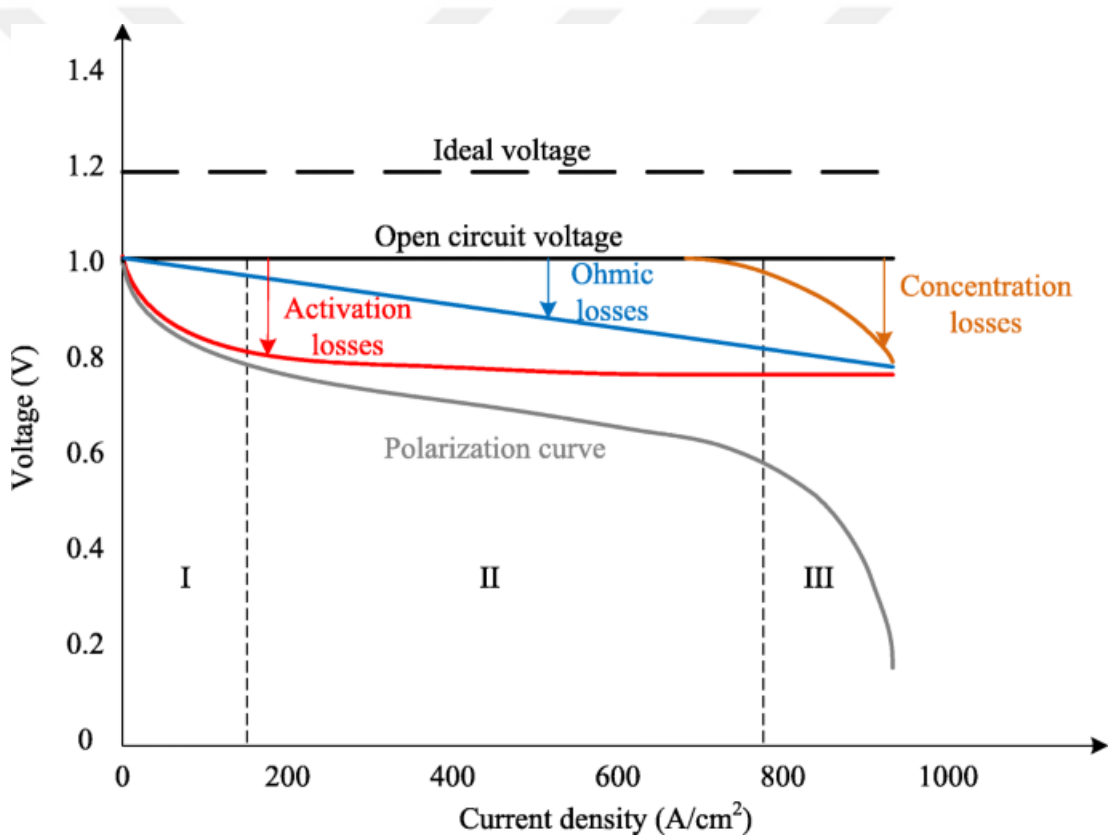

Figure 1.6 Cell voltage-current relationship illustrating the anticipated losses.

Irreversible losses that disturb the fuel cell performance are as follows:

- Ohmic losses (ΔV_{ohm}): These are the losses at intermediate current densities and caused by the ionic resistance of the electrolyte in the electrodes and other conductive parts within the fuel cell.

9

- Activation losses (ΔV_{act}): Losses here are essential for starting the reaction, related to sluggish electrode kinetics and also known as activation polarization.

- Internal currents.

- Mass transport losses (ΔV_{conc}): This type of loss occurs in high densities as it is entirely reliant on current densities.

- Crossover of reactants: A slight quantity of H_2 would diffuse from the anode to the cathode, while some electrons may also find a short track throughout the membranes. Although the electrolyte is not conductive, it is impermeable to gases.

Apart from these, other significant factors affect the practical H_2 equilibrium and open circuit voltages (OCV), namely the purity of the platinum coating on the gas diffusion layers, crossover, the corrosion of the carbon electrode support, etc. In-depth analysis is required to understand the effect of OCV on PEMFC performance. OCV is described as the voltage at zero current density, without any power output at the open-circuit condition. The values of OCV in PEMFC ranges between 0.9 and 1.1, lower than theoretical values (1.23 V) caused by the aforesaid main limitations, temperature, mixed potentials, hydrogen crossover, and the CHx impurities on the carbon support and Pt coating. Mixed potential on the cathode causes Pt oxidation, considered as one of the chief reasons for OCV drop in a PEMFC system. This phenomenon, i.e. when the H_2 and O_2 contact and react directly without losing electrons and proton, is known as H_2 crossover, and it is impossible to avoid gases from passing through the membrane without separating into H_2 and electrons, although the membranes are considered impermeable to gases. H_2 crossover increases with the decrease of the membrane thickness because of the high gas permeability of the membrane, thus resulting in minor OCV values.

1.5 PEMFC Main Components

1.5.1 Bipolar Plate

Bipolar plates are the backbone of HT-PEMFCs as they collect and conduct the electrons and provide the movement of reagents, H_2 and O_2. They are also referred to as 'flow field plates'. Multi-cell configurations involve very well-functioning bipolar

plates, whose key objective is to supply the reactive gasses to the core of the fuel cell through the flow channels. They also need to drain water efficiently. Graphite is the most common material used for bipolar plates owing to its outstanding electrical conductivity, high corrosion resistance, and lighter weight compared to materials such as steel or copper. These may also be used as bipolar plates, but their corrosion resistance is low and their density is more significant than graphite [19].

1.5.2 Gaskets

The gaskets are inserted in the PEMFC between the bipolar plates and the MEA to prevent the leakage of the reactant gasses and coolants from the flow channels into the cell. They also function as electrical insulators between the bipolar plates and the MEA, ensuring control of the stack height. Polymeric materials are commonly used as gaskets [22].

1.5.3 End Plate

The end plate is an important part of the PEMFC for a number of reasons, such as:
- Stacking of various other components (five-layer MEA, bipolar plate, gasket, current collector) of the stack.
- Serving as a flow channel to inlet the stack for reactant gases and coolant fluid.
- Applying equal pressure to the entire fuel cell to reduce ohmic resistance. Otherwise, proper electrical connection cannot be achieved and voltage drops occur in the cell.

The endplates are compressed with a certain degree of force from the edges for smooth and even pressure distribution – otherwise referred to as clamping force, which is equal to that needed to compress the stack and internal forces. The assembly pressure impresses the characteristics of the contact interfaces between the thin-scale components and the low mechanical strength of the fuel cell layers against the gaskets, bipolar plates, and the endplates. In case of inadequate or non-uniform clamping force, certain malfunctions can occur, such as fuel leakage, internal combustion, and high contact resistance. Excessive clamping force, likewise, also damages the stack, resulting in weathered porous structure and choking in the gas diffusion layer,

11

eventually reducing cell efficiency and speedy degradation. Each stack needs sufficient clamping power, depending on the fuel cell material and the stack design [23].

1.5.4 MEA (Membrane Electrode Assembly)

The MEAs, consist of two separate layers in the catalyst layer (CL) placement, known as the center of the PEMFC. Figure 1.7 shows the different MEA structures. In the first form, a catalyst ink applied to the Gas Diffusion Layer (GDL) leads to a standard two-layer structure [24]. This structure is called a Gas Diffusion Electrode (GDE). In the second structure, a catalyst ink directly coats both sides of the membrane. This structure, called the Catalyst Coated Membrane (CCM), forms a three-layer MEA. The third form of MEA comprises two GDEs sandwiched with a membrane or, alternatively, the CCM is sandwiched with two GDLs to form a five-layer MEA.
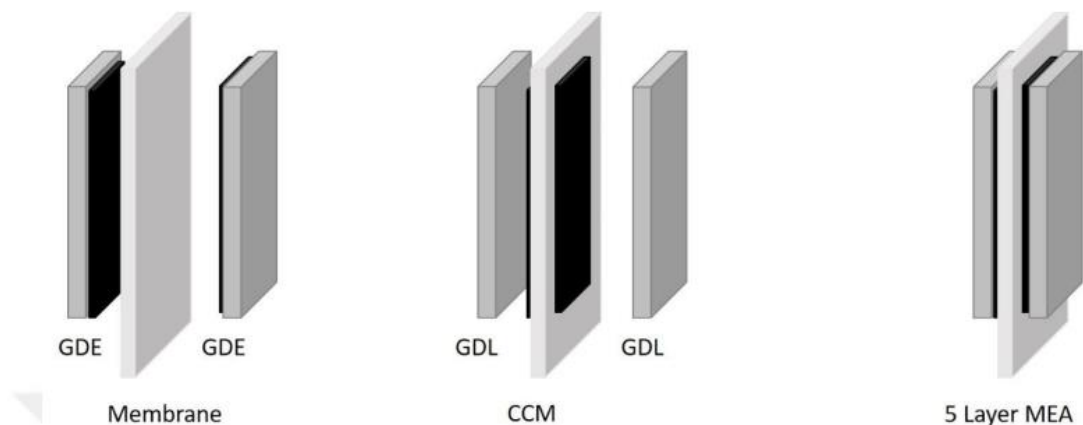
Figure 1.7 (a) MEA with GDEs and Membrane (b) MEA with GDLs and CCM (c) Five-layer MEA [25].

1.5.4.1 Gas Diffusion Layer (GDL)

The acceptable GDL for PEMFC has the following characteristics:

- Relative stability in the PEMFC environment;
- Elasticity under compression;
- High permeability for reactant gases and liquids; and
- Good electrical conductivity.

Generally, GDLs are classified into two main types: carbon paper or carbon fiber. While these varieties are similar to the area of use, they have different advantages and disadvantages due to their structural properties, which can significantly affect the transport of heat, current, gas, and water. Typically, they are made of porous composites, hence improved hydrophobic properties include binders such as polytetrafluoroethylene (PTFE) and carbon-based materials to enhance electrical conductivity. Besides, these added materials have a positive effect on the environmental issues of GDLs [26].

1.5.4.2 Catalyst Layer

Catalysts are used for H_2 oxidation and O_2 reduction reactions on the anode and cathode sides of the PEMFC [27]. The key functions of the catalyst are as follows:

- Maintaining an active reaction field.
- Serving as a conductive route for both the proton and the electron.
- Providing pores to allow the transfer of water and reagent gas.
- Containing an active triple-phase boundary where all reactants are mixed.
- Allowing for chemical stability under the conditions of pH and voltage.
- Tolerating reactant compositions.

1.5.4.3 Membrane

Polymer membranes have three primary functions in PEMFC [28].
- Charge carrier for protons;
- Separate the reactive gases; and
- Serve as an electronic insulator against the movement of electrons through the membrane.

In LT-PEMFC, the Nafion® membrane is a type of perfluorocarbon sulfonic acid and an excellent proton conductor with superior chemical stability, mechanical strength, and ionic conductivity, to mention a few [29]. Operations of Nafion® membranes at temperatures above 100 °C are adversely affected as the water required for the conductivity of the membranes evaporates in these settings [30].

In HT-PEMFC, the operations take place at higher temperatures in the range 100-200 ℃, attracting the attention of researchers due to significant advantages compared to LT-PEMFCs, for instance [31] [32].

- Catalyst poisoning is minimized, and higher CO tolerance makes it possible for a fuel cell to use hydrogen obtained from a reformer unit.
- The kinetics for both electrodes are improved; and
- Water is managed more easily and fuel cell flooding at the exhaust is avoided.

1.5.4.4 Classification of Proton Exchange Membranes

Polymer electrolyte membrane materials used in synthesis can be classified into three main groups [33].

- Perfluorinated and partially perfluorinated
- Non-fluorinated hydrocarbons, including aliphatic or aromatic structures
- Acid-based complexes.

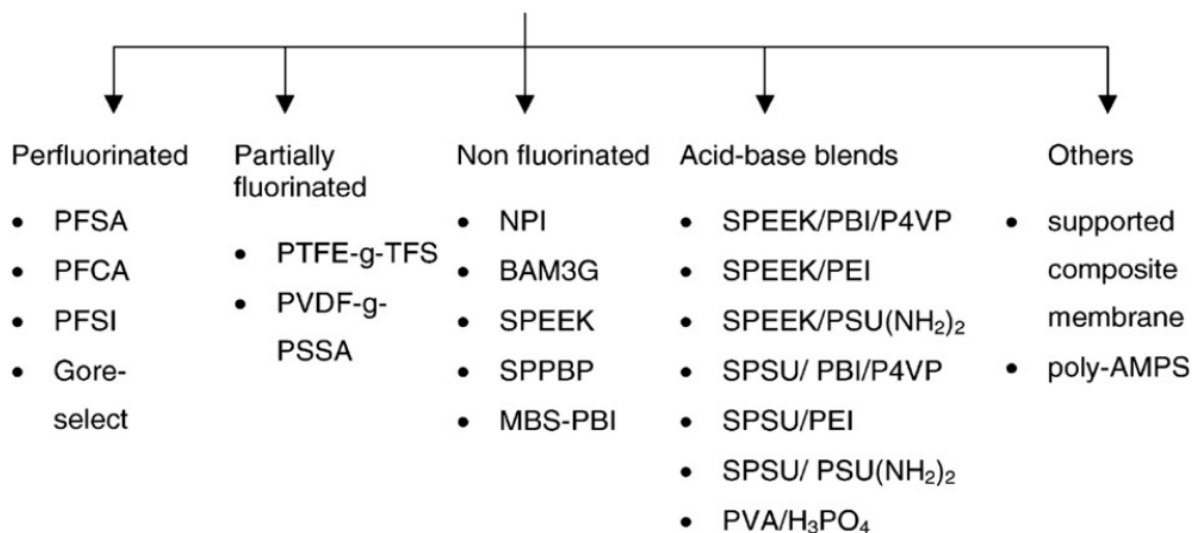| Perfluorinated	Partially fluorinated	Non fluorinated	Acid-base blends	Others
• PFSA	• PTFE-g-TFS	• NPI	• SPEEK/PBI/P4VP	• supported composite membrane
• PFCA	• PVDF-g-PSSA	• BAM3G	• SPEEK/PEI	
• PFSI		• SPEEK	• SPEEK/PSU(NH₂)₂	• poly-AMPS
• Gore-select		• SPPBP	• SPSU/ PBI/P4VP	
		• MBS-PBI	• SPSU/PEI	
			• SPSU/ PSU(NH₂)₂	
			• PVA/H₃PO₄	

Figure 1.8 Classification of proton exchange membranes based on perfluorinated, partially fluorinated, and non-fluorinated) materials and preparation method (acid-base blends and others) [28].

1.5.4.4.1 Perfluorinated Polymer Membranes

14

PPMs are chosen on the basis of thermostability, chemical inertness, and enhanced acidity of the sulphonic groups. Dupont's Nafion ® is the most renowned member of these membranes. Flemion ® by Asahi Glass and Aciplex-S ® by Asahi Chemical are two other related polymers. Additionally, Dow Chemical Company and Asahi Chemical Company have developed advanced perfluorosulfonic acids with shorter side chains and a higher ratio of SO_3H to CF_2 [34]. Figure 1.9 shows the chemical structure of Nafion® and other famous perfluorinated electrolyte membranes.

$$-(CF_2-CF_2)_x-(CF_2-CF)_y$$
$$(O-CF_2-CF)_m-O-(CF_2)_n-SO_3H$$
$$CF_3$$
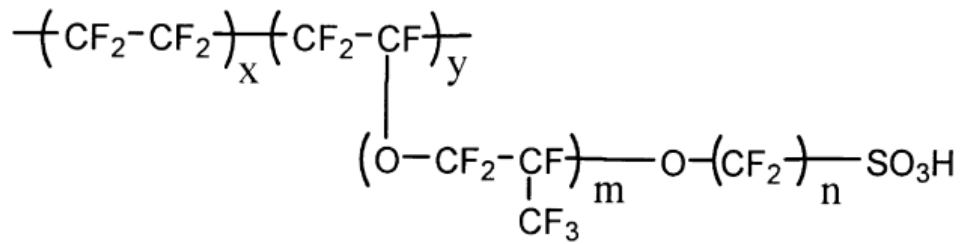
Nafion®117 $m \geqq 1$, n=2, x=5-13.5, y=1000
Flemion®   m=0, 1; n=1-5
Aciplex®   m=0, 3; n=2-5, x=1.5-14
Dow membrane   m=0, n=2, x=3.6-10

Figure 1.9 Chemical structures of perfluorinated polymer electrolyte membranes [35].

In the 1970s, DuPont introduced a perfluorosulfonic acid called Nafion ®, known to be superior to others due to its high proton conductivity, chemical stability, and mechanical strength[36]. It showed a twofold increase in the proton conductivity and a fourfold increase in the lifetime of the PEMFCs. It is now known as a standard and the most widely used type of membrane today. Nafion® is composed of fluoro 3,6-dioxo 4,6-octane sulfonic acid with polytetrafluorethylene (PTFE). The Teflon backbone of this structure gives a hydrophobic nature to the membrane, while sulfonic acid groups are added to the membrane, where the conductivity of the proton – a key parameter affecting the efficiency of the PEMFC - is directly affected by the hydration membrane level.

1.5.4.4.2 Non-fluorinated Hydrocarbon Membranes

15

Another type of material often used in PEMFCs is the non-fluorinated membrane. Hydrocarbon polymer membranes can be aromatic or aliphatic with benzene rings in the backbone or bulky pendant groups of polymeric spine membrane. Hydrocarbon polymers are widely researched due to the promising results of high-performance membrane production [37]. They are cheaper and commercially available, while their structure is suitable for adding polar sites as pendant groups [33].

To raise membrane stability at elevated temperatures, aromatic hydrocarbons may directly introduce the backbone of hydrocarbon polymers or polymers with bulky groups added as a modification. Polyaromatic amines have a rigid, bulky group and, thus, a Tg value greater than 2000 ℃.

1.5.4.4.3 Acid/Base Polymer Membranes

In the same way, acid-base complexes have been considered a suitable alternative for membranes that can support high conductivity at elevated temperatures without facing dehydration effects. Generally, these complexes are considered for fuel cell membranes incorporating an acid element within an alkaline polymer base to promote the conduction of the proton. In the absence of free water, pure sulphuric and phosphoric acids are self-ionized. Polymers containing primary sites such as alcohol, ether, and amine, amide, or imide groups react with strong acids and increase acid dissociation. The polymer studied in earlier years includes polyethylene oxides (PEO) [38], polyvinyl acetate (PVA) [39], polyacrylamide (PAAM) [40], polyvinyl pyridine (PVP), and linear & branched polyethyleneimine (L- or B-PEI) [41]. Phosphoric acid has good conductivity and thermal stability, known to perform well in phosphoric acid fuel cells (PAFCs) at intermediate temperatures between 175°C–200°C. Conventional PAFCs, on the other hand, have limited applications due to the disadvantage of electrolyte phosphoric acid immobilization in some matrices. So far, though, the phosphoric acid-doped polybenzimidazole (PBI/H_3PO_4) method continues to be the most competitive temperature membrane between 175°C–200°C. Fuel cell technologies based on the PBI/H_3PO_4 method have been successfully introduced at these temperatures under atmospheric pressure. Gas humidification is not needed and the Pt-based catalyst, CO sensitivity is better at higher temperatures. PBI /H_3PO_4 systems, as typical membranes for HT-PEMFCs, are the most promising candidates.

Easy management of the airflow rate and cell temperature is another operational feature of the PBI-based fuel cells [34].

1.6 Proton Conduction Mechanisms in PEM

Proton conduction has an important significance in many chemical reactions, bio-molecular and electrochemical energy transfer processes. The exceptional proton chemistry indicates two mechanisms for proton conduction: proton transfer by a carrying molecule (vehicle mechanism) or utilizing a hydrogen bond chain hopping from one site to another one (Grotthus mechanism) [42]. In the vehicle mechanism, the protons transfer with a molecular transporter without an infinite hydrogen bond web, thus following Stokes Theory. Water is the most common proton solvent, and proton conducting of different hydrated proton complexes in aqueous media also requires a migration. PFSA membranes consist of the sulfonic acid functional groups of a perflourized backbone and perfluorinated functional groups. High fluorine electronegativity tends to super close interactions between the sulfonic acid and the perfluorinated backbone. It absorbs water, which contains the protons domain developed for continuous hydration. The protonic carrier charge is the resulting hydrated protons [43]. This phenomenon primarily depends on a vehicle mechanism as described earlier, as well as the degree of hydration of the membrane, which induces PSFA proton conductivity. These membranes have proton conductivity values above 0.1 S cm^{-1} under totally hydrated conditions [44]. The process of Grotthus includes a hydrogen bone web, and the hydrogen bond strength is roughly intermediate at 10-30 kJ mol^{-1}.

As the bond strength is comparatively low, several different factors, such as thermal energy, may cause hydrogen bonding to form and break down. This dynamic formation is ideal for the hopping of the proton conduction process. The hopping process consists of splitting an O-H bond within one molecule and creating the same sort of bond with another molecule. Each proton travels over very minimal distances, but a load movement takes place at a longer distance. In comparison to typical ion motions through viscous material, the activation energy of this phase is lower than that of the regular movement of ions through viscous media. A membrane of this type of proton conduction mechanism is needed to achieve higher temperature operations with PEMFCs.

17

In this context, the most promising results have been obtained by doping simple amphoteric acid polymers, such as phosphoric acid doped PBI systems. Studies have shown that the conductivity of the membrane strongly depends on the acid content of the two materials. Minimum conductivity is measured at the acid degree leading to maximum protonation. To achieve higher conductivity values, excess acid is required. This indicates that proton conduction proceeds mainly through the hydrogen-bonded anion chain. The conductive mechanism of the proton remains the same, mostly by the Grotthus mechanism. However, the rotational motion of the phosphoric acid molecules required for this mechanism is limited by PBI-H_3PO_4 interactions. This results in a lack of proton conductivity as protons are not effectively protonated between proton imidazole (ImH+) and H_3PO_4 [44].

CHAPTER 2

LITERATURE SURVEY

2.1   Acid Doped Polybenzimidazole Membrane

PBI (poly [2,2-m-phenylene)-5,5-bibenzimidazole]) has been introduced as a possible replacement for Nafion; it is a linear heterocyclic polymer containing a benzimidazole nucleus as a repeat unit of amorphous thermoplastic polymers [45]. PBI has high thermal stability (Tg= 425- 436℃), high chemical resistance, and retention of stiffness as well as toughness. Another common form of polybenzimidazole, known as ABPBI, has a very similar structure to that of PBI, but it does not have a connecting phenyl group.
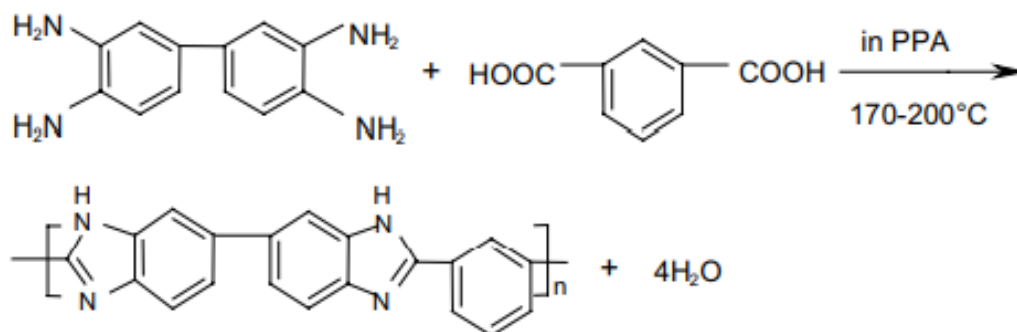
*X: -COOH, -COOCH$_3$, -CONH$_2$ or –CN

Figure 2.1 Polybenzimidazole synthesis by solution polycondensation [46].

In 1961, Vogel and Marvel first synthesized PBI by melting polycondensation [47]. The synthesis of certain polymers is based on the condensation of tetraamines and diacids. Polycondensation solution was later suggested to produce high-molecular PBI weight. Temperature management was found to be simpler in the latter method because PPA was used as a solvent in there and the reaction temperature was lower, about 170-200℃. This process is an excellent route for the preparation of laboratory or small-scale PBI polymers (Figure 2.1). PBI polymer can be solved in different organic solvents among which DMAc is one of the most common. A solvent casting technique for membrane preparation includes solving PBI polymer in a DMAc solution, then fed onto a flat surface to dry. The solvent concentration ranges from 2.5 to 20 wt. %. If the concentration is too low, the breakdown of the polymer chain of PBI is not enough to create stable membranes. Conversely, that is if the solution is too concentrated, it would be difficult to achieve a homogeneous solution [48]. Compared to the solution cast PBIs, direct cast para-PBIs show a fully amorphous structure and higher acid doping levels [49]. Sulfonated polybenzimidazoles have also been studied in the literature widely [50]–[53]. and membranes developed with them are used in sensors [56], and electronic devices [49].

PBI is not a conductive polymer, but doping it in strong acid turns it into an efficient proton conductor. Different types of acids have been investigated, revealing that phosphoric acid (H$_3$PO$_4$) and sulfuric acid are more suitable for the use of HT-PEMFC. Phosphoric acid has high thermal stability, making it a desirable candidate for PBI acid doping as a key process to determine how the PBI membrane behaves as a PEM. Doping involves imbibing the membrane in phosphoric acid yield 5-16 mol of H$_3$PO$_4$ per mole PBI repeat unit. In 1995, Wainright et al. developed the first adopted H$_3$PO$_4$ - doped PBI membranes for polymer electrolyte membranes (PEMs) [57]. Over the past 20 years, intensive research has been carried out to enhance the commercial development of acid-doped PBIs. These polymers have also been imbibed with other acids [58], bases, and inorganic proton-conducting molecules [59]. PBI doped with H$_3$PO$_4$ increases the performance of the membrane up to several magnitudes in terms of conductivity. Nevertheless, PBI membranes also have tech-

nical limitations in H_3PO_4 because of: (1) poor mechanical characteristics caused by high doping levels; (2) agglomeration in the catalyst particles; and (3) membrane acid release, in particular at high temperatures and humidity levels [60]. This leads to loss of conductivity of the proton in the membrane and a severe corrosion problems [61]. To tackle this problem, certain approaches have been introduced in the literature.

2.2 Previous Studies on Composite Membranes

The idea of forming composite membranes is based on utilizing polymer materials, namely Nafion, polyether ketone, polybenzimidazole, and the like, as a matrix and some inorganic crystals as filler. The preparation of composites with inorganic fillers has been the focus of recent attempts to develop better-performing PEMs. In the same way, the addition of hygroscopic filler to ionomer has been shown to improve water and acid retention to make the membranes stiffer. An inorganic filler can also increase thermal resilience, water absorption, reactant crossing resistance, etc. in the membrane matrix [62].

One of the critical guidelines in developing PBI-based materials is combining the organic matrix with an inorganic material to increase the functional properties of the membrane. The development of composite membranes has been widely studied in literature to solve the acid doping and acid leaching problems. Many forms of fillers have been investigated, among them clay [63], graphene [64], [65], and silica particles [66]. Conductive inorganic proton like zirconium phosphate, phosphotungstic acid [67], silicontungstic acid [68], and boron phosphate [69] have been studied with PBI matrix. have also been studied with the PBI matrix, showing that higher conductivity values, up to 0.2 S cm^{-1} could be obtained by adding inorganic proton conductors [70].

Devrim et al. prepared a PBI/SiO$_2$ hybrid membrane with improved acid uptake, retention property, and proton conductivity owing to the good interaction between the PBI polymer and SiO$_2$. The highest proton conductivity (0.1027 S/cm at 180 ℃ and 0 % RH) [71]. Lobato J. et al. prepared a novel PBI-based composite membrane with a titanium oxide composite membrane that showed high conductivities at all temperatures and high doping. This finding indicates that the presence of an inorganic

filler makes a significant contribution to the PBI membrane structure, thus leading to better performance for the composite membrane [72]. Uregen et al. prepared PBI/GO composite membranes with different weight percent loadings of GO by means of the solution blending method, leading to a maximum proton conductivity at 0.1704 S/cm for PBI/GO with 2 wt. %. This research demonstrated the possibility of promising PBI/GO composite membranes for HT-PEMFC [73]. Ozdemir Y et al. prepared PBI-based composite membranes with different fillers, such as TiO_2, SiO_2, and ZrP, successfully prepared and characterized for HT-PEMFC application, The results show the importance of the inorganic particles for gaining adequate chemical, thermal and mechanical stability [70]. Kanna et al. improved performance of phosphonate carbon nanotube–polybenzimidazole composite membranes. using The main advantage of using composite membranes based on PBI and phosphonated MWCNTs for PEMFC application is demonstrated as a unique opportunity to enhance proton conductivity, stability, and overall performance [75]. Lin et al. prepared PBI-PTFE composite membranes. Nafion-covered PTFE is used as a filler matrix, where Nafion serves as a coupling agent by an acid-base reaction with PBI. The thickness of the membrane was low as 22 μm; also, the gas permeability of the membrane was low [76]. Muthuraja et al. prepared $NanoCaTiO_3$ by the sol-gel method, and incorporated it into the synthesized m-PBI membranes to form nano CTO-PBI composite membranes. The acid doping was improved with an increase of nano CTO content [77]. Plackett et alPlackett et al. prepared organo-modified laponite clays by ion-exchange. High levels of acid doping in the composite membranes could be accomplished while maintaining adequate mechanical strength. With much decreased acid swelling, the robust composite membranes became more dimensionally flexible, expected to increase the durability and performance of the fuel cells [78]. Moradi et al prepared PBI-Fe_2TiO_5 nano-composite membranes with 4 wt. percent of nanoparticles and the best values for PA doping was 12 and for proton conductivity at 0.078 S/cm. In addition, in order to predict the conductivity of the PA-doped PBI-Fe_2TiO_5 (PFT) nano-composite membranes, a semi-empirical model was developed for the effects of phosphoric acid doping [79].

Table 2.1 Previous studies on composite membranes.

Membrane	Filler wt. (%)	Proton Conductivity (S/cm)	T (°C)	Fuel cell performance max power (W/cm)	T (°C)	Acid Doping	Ref.
PBI/SiO$_2$	5	0.1027	180	0.250	165	10	[71]
PBI/TiO$_2$	2	0.180	125	0.80	150	15.3	[72]
PBI/GO	2	0.170	180	0.38	165	13	[73]
PBI/ZrP	5	0.200	180	-	-	15.4	[70]
PBI/TiO$_2$	5	0.044	140	-	-	13.6	[70]
PBI/SiO$_2$	5	0.113	180	-	-	13.4	[70]
PBI/p-MWCNT	1	0.11	160	0.78	140	12	[75]
PBI/PTFE	18.7	0.133	150	0.570	180	38	[80]
PBI/CaTiO$_3$	10	0.028	160	0.57	160	127%	[77]
PBI/laponite clay-N	15	0.120	120	0.22	150	8.2	[78]
PBI/CsPOMo	30	0.120	150	0.6	150	45	[81]
PBI/Fe$_2$TiO$_5$	4	0.078	180	0.430	180	12	[79]

2.3 Boron Nitride as Filler

The structural formation of Boron Nitride (BN) depends on boron and nitrogen atoms in the direction of the lattice plan. These structures are amorphous, hexagonal, cubical, and root-shaped. Nanomesh, boron nitride and aerogels are also present in several biomedical applications [82]. Initially, boron nitride was developed in the early 18th century, but it remained out of wide use until the 1940s. Today, it is mainly formed by reacting with ammonia (or sometimes urea) on boron trioxide or boric acid in a nitrogen atmosphere. What makes boron nitride unique is its similarity to the most versatile element, carbon, which shares the same number of electrons between the adjoining atoms in the electronic structures. The two most popular types of boron nitride are graphite and diamond equivalents. Just like synthetic diamonds are made from graphite, the diamond-like cubic boron nitride is produced from the basic hexagonal version by applying extreme pressure and temperature. The result is crystals that are almost as hard as diamonds and beat their hands on some other capabilities with their carbon brethren [83].
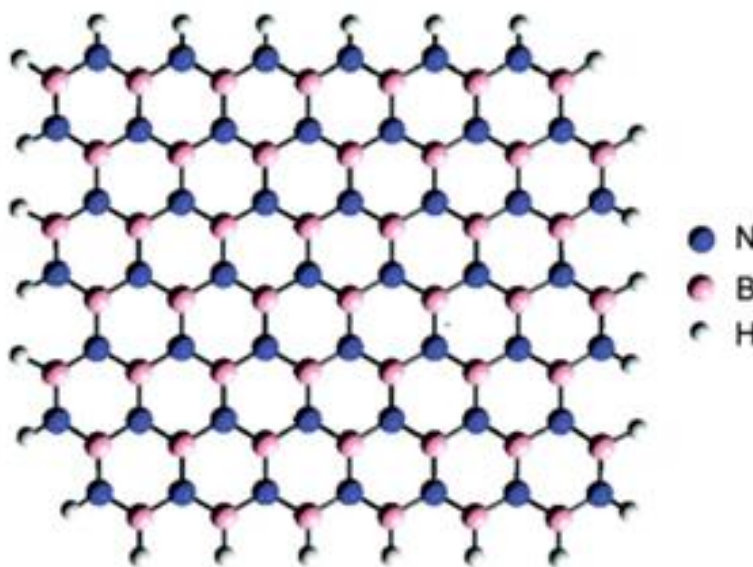

Figure 2.2 Hexagonal Boron Nitride structure.

Hu et al. showed that hexagonal boron nitride is an excellent proton conductor (Figure 2.2) at room temperature with a monolayer h-BN; at higher temperatures, h-BN

is outperformed by [84]. Further research has shown that the rates of h-BN increase in the exponential plot of the Arrhenius type with increasing temperature compared to graphene rapidly increase [85]. These results can be a step forward in improving fuel cell performance and, perhaps, even a substitute for perfumed membranes, e.g. Nafion, which has several disadvantages. An isostructural of covalently-bound alternating boron and nitrogen, h-BN makes its way to sophisticated applications [86]–[89]. Boron nitride (BN), Often known as "white graphene", a large band gap in h-BN makes it an electrically insulating material with excellent mechanical and thermal properties making it a viable filler material for polymer composites [90]–[93]. A reasonable proton conductor should be an ideal polymer electrolyte membrane with electrical insulator properties [94]. H-BN is only in its early stages as a composite membrane filler used in fuel cells. There have been very few efforts to evaluate the use of h-BN in polymers composite [89], [95]. H-BN provides the polymer with thermal and mechanical strength when incorporated in the matrix [96]. while its high surface area also makes it a good absorbent for organic pollutants, dyes etc. [97]–[99]. Hu et al. found that h-BN is an excellent proton conductor, referring to the highest proton conductivity at room temperature and higher with a monolayer h-BN [84].

2.4 Aim of the Study

In this thesis, BN is selected as a filler to prepare a PBI composite membrane owing to its advantages, namely good thermal resistance and high stability. As stated earlier, there are not enough studies in the literature on BN-doped PBI membranes. The prepared PBI/BN composite membranes developed in the present study are characterized using TGA, SEM, acid doping and acid leaching techniques. To determine the suitability of the BN materials, the prepared composite membranes are evaluated by ex-situ electrochemical investigations and in-situ HT-PEMFC.

CHAPTER 3

METHODOLOGY

3.1 Materials

Polybenzimidazole (PBI) was obtained from Danish Power System (Denmark). Polyphosphoric acid (PPA) (115% phosphoric acid equivalent), N-N dimethylacetamide ($CH_3C(O)N(CH_3)_2$ DMAc) phosphoric acid ($H3PO4$, 85 %), polytetrafluoroethylene (60 wt. % dispersion in H_2O), 2-propanol and deionized water were purchased from Sigma Aldrich (USA). Boron Nitride (BN) nanoparticles, purity: 99.85+%, size:65-75 nm, Hexagonal were purchased from Nanografi Nano Technology (Turkey). Pt/C catalyst (60 wt. Pt %) and carbon paper gas diffusion layer (with a micro-porous layer) were purchased from Johnson Matthey (United Kingdom) and Freudenberg (Germany), respectively. The high purity H_2 and N_2 gases were purchased from Linde Gas (Turkey). All the chemicals were of analytical reagent grades and used as received, without further purifications.

3.2 Membrane Preparation

In this study, PBI-based composite membranes were prepared with BN as an inorganic filler. The PBI composite membranes were obtained by the solvent casting method; to do so, firstly the PBI membrane was dissolved in DMAc at atmospheric pressure at 80 ^{o}C temperature. Then, proper amounts of the inorganic particles (2.5-10 wt. % BN) were dispersed by ultrasonication in the PBI polymer solution to obtain a homogenous solution, which was then cast onto a petri dish and DMAc evaporated in a ventilated oven at a temperature of 100 ^{o}C for 24 h. the prepared composite membrane was stripped from the petri dish. The PBI membrane without filler was also prepared with the same procedure for comparison. All membranes were doped in H_3PO_4 for two weeks to maintain acid doping and proton conductivity.

.
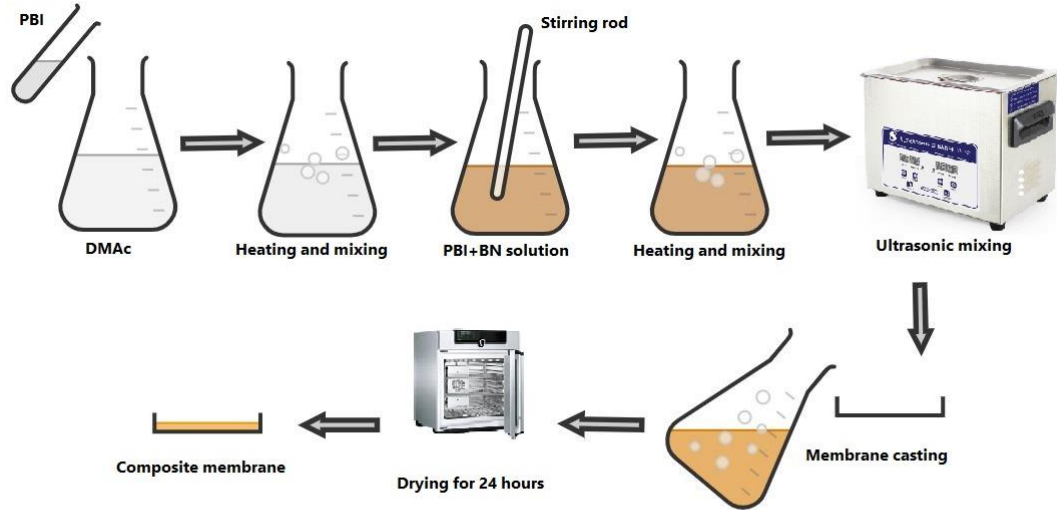
Figure 3.1 Membrane preparation procedure.

3.3 Acid Doping of the Membranes

To maximize proton conductivity, the PBI matrix requires a significant amount of H_3PO_4 integration. The acid was absorbed in the matrix due to the strong interaction between PBI and PA [71]. The membranes were soaked in a H_3PO_4 solution and the membranes weight was determined before and after doping, with the respective values calculated according to the following Equation (10). Accordingly, the doping level of the membrane refers to the number of H_3PO_4 moles per PBI repeat unit.

$$\text{Acid doping} = \frac{W_{PA}}{W_{dry}} \times \frac{\text{MW of PBI repeat unit}}{\text{MW of } H_3 PO_4}$$

(10)

where W_{PA} is the weight of the acid doped membrane and W_{dry} is the dry membrane weight [100]. Membrane thickness was obtained as ~50μm after acid doping.

3.1 Characterization of Membranes

3.1.1 Thermal Gravimetric Analysis

The thermal stability of the membranes examined using a Thermal Gravimetric Analyzer. The temperature range was 20°C - 950°C, at a heating rate of 10°C/min under a nitrogen atmosphere.

3.1.2 Acid Leaching Tests

The membranes were kept in direct contact with water vapor for 5 h, and weight loss due to the PA leaching of the membrane was determined by measuring the membrane weight every hour. The percentages of acid leaching of the membrane are determined according to the following Equation (11):

Acid Loss Percentage $= \dfrac{W_{PA\ doped} - W_{initial}}{W_{acid}} \times 100\ \%$

(11)

3.1.3 Mechanical Tests

Tensile tests were carried out to assess the mechanical performance of the membranes. These measurements were performed in compliance with ASTM 638. An Instron 3367 universal test machine was used (Figure 3.4) and the test speed was determined as 5 mm/min. For the test, dog-bone-shaped samples were cut and examined using a universal tensile test machine. Load (F) was applied to the dog-bone-shaped sample gripped symmetrically. With the help of an extensometer, the change in the length of the specimen (Δl) was measured with the original length as reference (l_0).
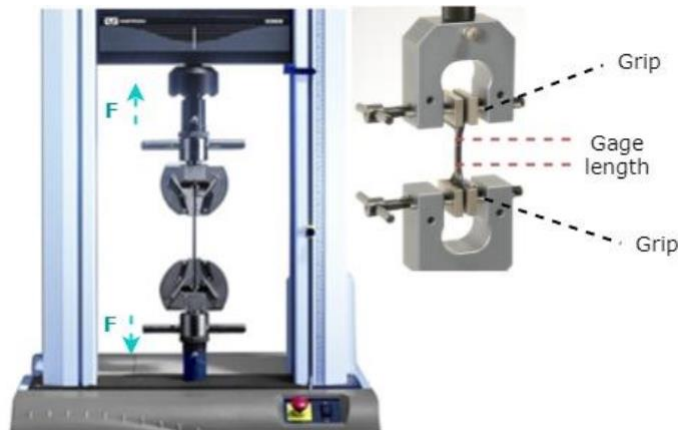

Figure 3.2 The Instron 3367 tensile machine and a representative apparatus [101]**.**

3.1.4 Scanning Electron Microscopy Analysis (SEM)

The morphologies of the composite membranes were examined using a Scanning Electron Microscope (SEM) and QUANTA 400F Field Emission SEM system equipped with an energy dispersive X-ray (EDX) spectrometer. All the membrane samples were quenched in liquid nitrogen, subsequently leading to their fracture. Later, these fractured surfaces were coated with a layer of gold to avoid charging during the SEM analysis. Surface SEM analysis was conducted using a Zeiss Evo LS15 microscope for the PBI/BN-2.5 composite membrane.

3.2 Proton Conductivity Measurement

The proton conductivity of the composite membranes was measured using a four-probe method with a ZIVE SP2 electrochemical workstation test device. As the term implies, the method consists of four equal spaces (1 cm) for each Pt probe. The membranes are cut to fit into the measuring cell to interact with all four probes. The AC impedance for all membranes was measured between 65 MHz and 65 MHz. Subsequent measurements were performed at three different temperatures as 140°C, 165°C, and 180°C, and data was collected for approximately one hour for 10 to confirm their relativity at each temperature. The results fitted the Randel's Circuit model, which was available in the software database to devise polymer models. The experimental set-up used for proton conductivity analysis is given in Figure 3.7.
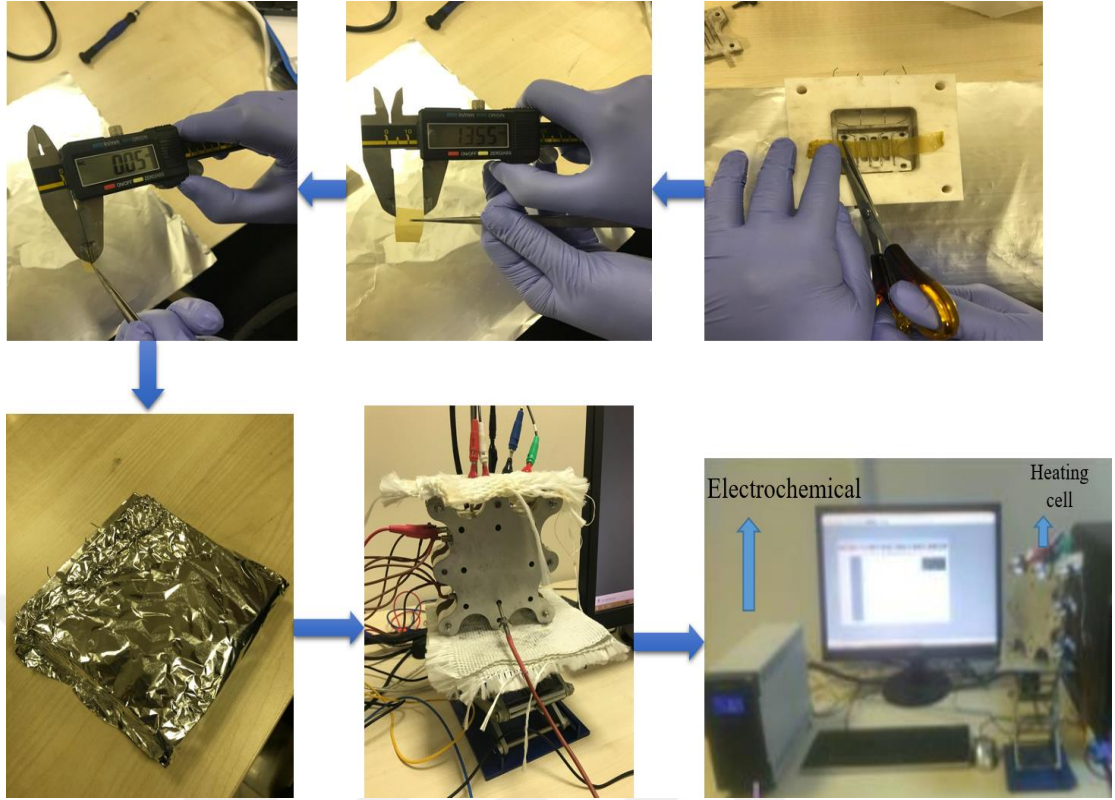
Figure 3.3 Experimental set-up for proton conductivity analysis.

The conductivity of the membranes was calculated using the following Equation (12).

$$\sigma = \frac{L}{r \times w \times t} \tag{12}$$

where σ is the proton conductivity of the membrane (S/cm), r is the Rs (resistance) value obtained for the membrane (Ω) from the software output, w is the membrane width (cm), t is the membrane thickness (cm) and L is the gap between two probes of the impedance cell (cm).

3.3   Preparation of Membrane Electrode Assembly

The membrane electrode assemblies (MEAs) were prepared by spray coating technique. For this, Pt/C was used as an anode and cathode-side catalyst. The commonly preferred Nafion polymer binder in LT-PEMFC is not suitable for HT-PEMFCs operating at higher temperatures due to the non-humidified conditions [102]. For this reason, PTFE was applied as a binder to avoid acid stripping in the electrodes and to increase interaction with the membrane. The catalyst ink was composed of a Pt/C

catalyst, Teflon solution (PTFE), deionized water and 2-propanol. For ink preparation, firstly the Pt/C catalyst was mixed with deionized water, and then 2-proponal and the PTFE solution was added. The resulting solution was placed in ultrasonic mixing for 40 min. After that, GDL was coated with the prepared catalyst ink with a spray gun, as shown in Figure 3.5. The catalyst loadings at the anode and cathode were kept constant at 1 mg_{Pt}/cm^2. The prepared GDE was placed in an oven at 90℃ for 24 h. Finally, GDEs were pressed onto both sides of the H_3PO_4 doped membrane at 150 °C and 172 N/cm^2 for 10 min with a hot press in the Hydrogen Energy and Fuel Cell Research Laboratory at Atilim University (Figure 3.6). Prepared MEAs were placed in closed vessel to protect from air humidity.
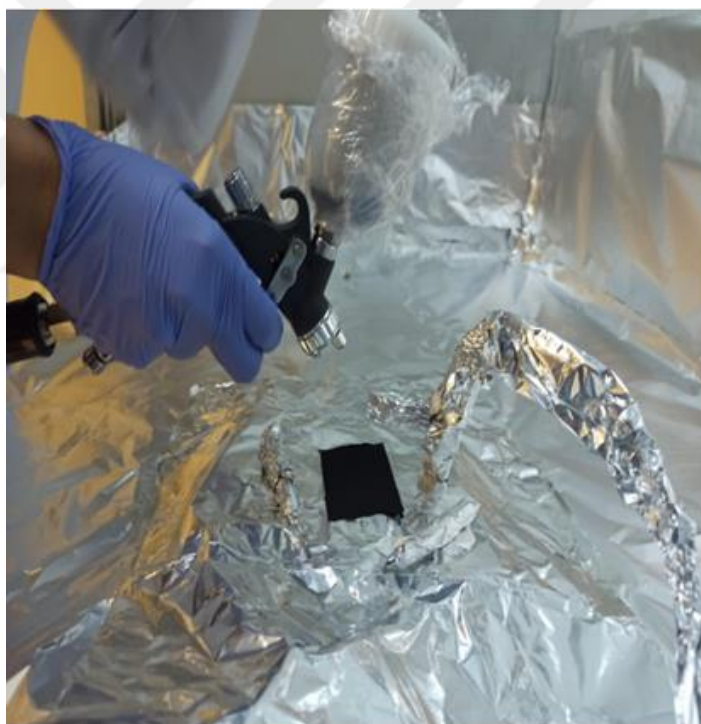
Figure 3.4 GDL coating with spray gun.

Figure 3.5 Hot press.

3.4 HT-PEMFC Test

The HT-PEMFC tests were examined to assess the high-temperature PEMFC performance of the composite membranes. Measurements were carried out at the HT-PEMFC (TECHSYS) test station at the above-stated laboratory (Figure 3.6). MEAs were tested in an HT-PEMFC single-cell with an active area of 5 cm^2. The flow field plates were made of graphite and the serpentine type made up the geometry of the flow channel. Single-cell HT-PEMFC sealing is an essential parameter since oxygen and hydrogen would be mixed if the sealing failed, leading to MEA burning [103]. To avoid sealing failures and mixing of the reactant gases, Viton gaskets were applied. Also, due to the low active area the single HT-PEMFC temperature was maintained at working temperature by externally heating the end plates.
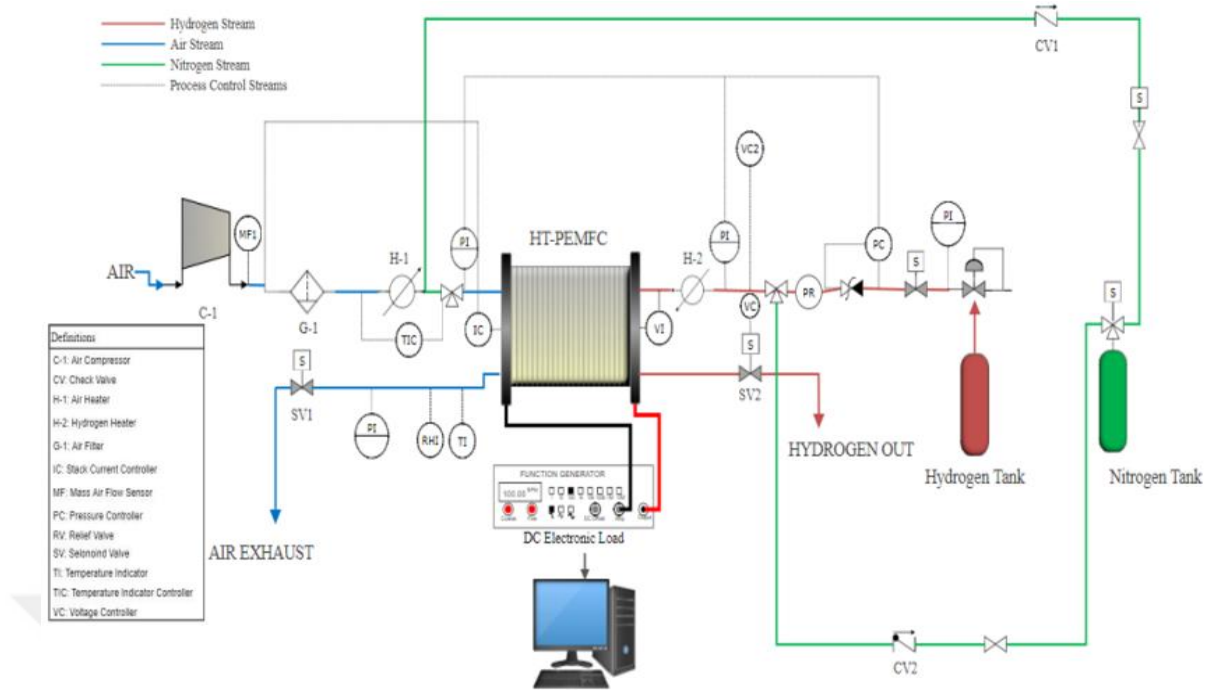
Figure 3.6 The HT-PEMFC Test Station.

The test was performed with the following reactant gas flow rates and stoichiometric ratios:

- H_2: 0.05 slpm, at 1.5 stoichiometry (%99.995 H_2).
- Compressed Dry Air: 0.12 slmp, at 2.5 stoichiometry directly fed from compressor/dryer.

After MEA conditioning for 5 h at 0.6 V, the efficiency of the fabricated MEAs was evaluated. The cell current and voltage were monitored and logged by the fuel cell test software during the cell operation. The current-voltage data were collected by changing the voltage values from the load values until steady-state was achieved, beginning with the OCV value.

CHAPTER 4

RESULTS AND DISCUSSION

4.1 Thermal Gravimetric Analysis

The thermal stability of the composite membranes was examined to measure the effect of BN fillers on the thermal property of the PBI membrane. The TGA analysis was conducted by heating the membranes first from room temperature to 100℃. The membranes were then held at 100℃ and heated to 900℃ with a rate of ramping of 10℃/min and a dry flow of N_2. Figure 4.1 shows the TGA analyses results of the PBI and composite membranes with different amounts of BN filler.

Figure 4.1 TGA analysis of the PBI/BN composite membranes.

According to the results, the pristine PBI membrane showed good thermal stability up to 600°C [100]. The main weight loss was determined at 100-200 °C and attribut-

ed to bound water and remaining solvent. Additionally, all PBI/BN composite membranes showed similar thermal stabilities and, as seen from figure, the weight loss up to 2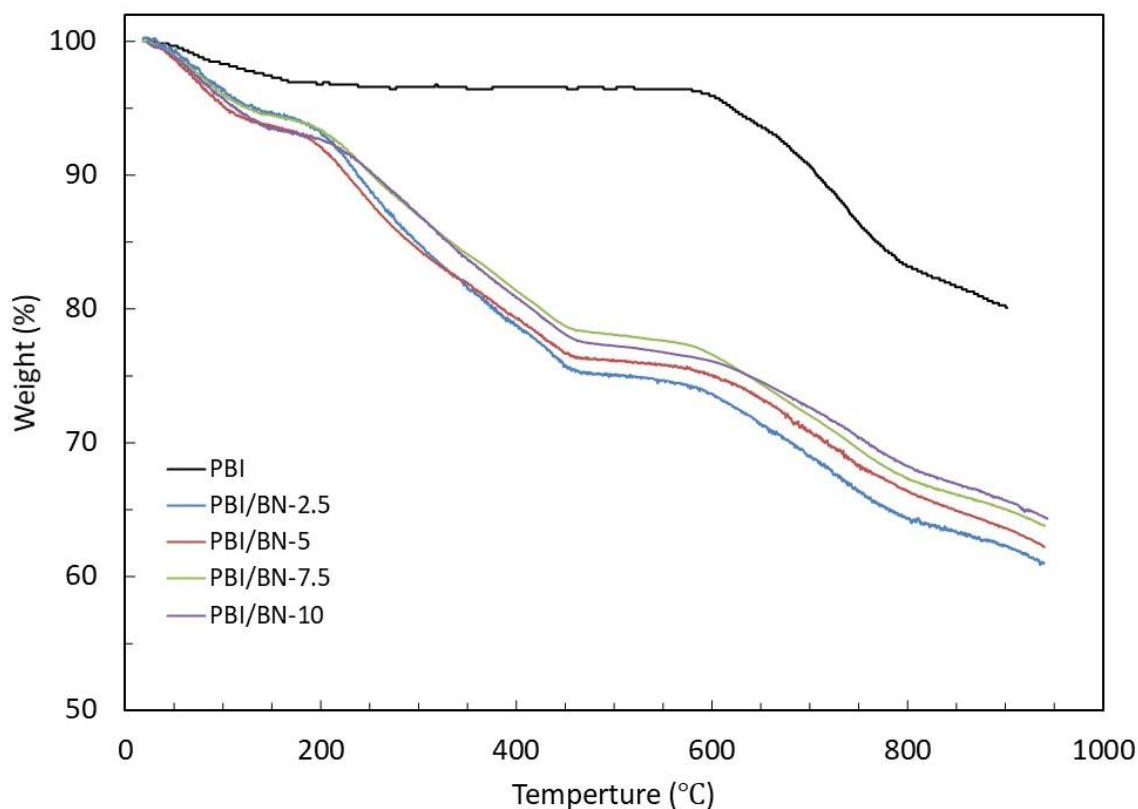00 ℃ can be related to the water and remaining solvent as PBI. The second weight loss region was observed between 200-400°C for the PBI/BN membranes. Decomposition temperatures were found at 587 ℃ for PBI/BN-2.5 wt.%, at 601 ℃ for PBI/BN-5.0 wt.%, at 614 ℃ for PBI/BN-7.5 wt.%, and at 638 ℃ for PBI/BN-10 wt.%. Excluding the loss of the volatiles, no significant weight loss was observed for the membranes prepared up to 200℃, which is high enough for fuel cell applications. All the membranes prepared are thermally stable at the fuel cell operating temperatures. Therefore, they can be used in HT-PEMFC applications.

4.2 Acid Doping

As stated previously, the purpose of H_3PO_4 doping of the membranes is to maintain proton conductivity. To this end, all membranes were doped as such, as indicated in Table 4.2 for acid doping levels (ADLs). The pure PBI membrane ADL was obtained as 12.7 number of H_3PO_4 moles per PBI repeat unit. According to the obtained results the ADL values were 12.9, 11.7, 10.8 and 11.2 for the number of H_3PO_4 moles per PBI repeat unit as PBI/BN-2.5, PBI/BN-5, PBI/BN-7.5 and PBI/BN-10 composite membranes, respectively. The ADL was increased up to 2.5 BN content. However, the increase in the BN constant within the polymer matrix decreased ADL due to the self-aggregation of the BN particles, leading to reduced nanoparticle surface [79].

4.3 Acid Leaching

Acid leaching experiments were performed to determine the acid retention ability of the composite membranes. The procedure as indicated in the literature was used to determine the effect of inorganic particles used on acid leaching [50]. whose values appear in Table 4.4. Accordingly, these values for PBI, PBI/BN-2.5, PBI/BN-5.0, PBI/BN-7.5 and PBI/BN-10 membranes were obtained as 83.5, 70.9, 72.3, 76.7 and 75.6 %, respectively. It can be seen that all PBI/BN membranes have lower acid leaching levels compared to the PBI membrane. Because of the hydrophilic nature of the nanoparticles of BN [104], they act as trappings for phosphoric acid inside the nanocomposite membrane structure, thus preventing H_3PO_4 leaching within the membranes.

4.4 Proton Conductivity Analysis

The proton conductivity measurements of the membranes were performed in the longitudinal direction at dry conditions with four probe EIS as a function of the temperature. The respective values appear in Table 4.1, based on which the top value was observed for PBI/BN-2.5 as 0.260 S/cm at 180 ℃ which also has the highest acid doping 12.9 and the lowest acid leaching 70.9 %. Within the same conditions, the proton conductivities of PBI, PBI/BN-5.0, PBI/BN-7.5, and PBI/BN-10 were 0.085 S/cm, 0.179 S/cm, 0.092 S/cm, and 0.125 S/cm, respectively. Major proton transport is carried out with hexagonal BN and H_3PO_4 groups.

From the literature, high proton conductivities for PBI membranes with high H_3PO_4 doping levels were collected. Accordingly, Ozdemir et al. obtained proton conductivity as high as 0.200 S/cm by using an inorganic proton conductor zirconium phosphate (ZrP) as a filler [70]. Pu et al. proposed that proton transport in H_3PO_4 doped PBI is a result of two contributions: one is fast proton exchange (hopping); and the other one is the self-diffusion of phosphate moieties and water molecules (vehicle mechanism) [105], [106]. The reduction in proton conductivity for PBI/BN-7.5 can be justified by considering the agglomeration of BN particles.

Table 4.1 Proton conductivity results with acid doping and acid leaching results.

Membrane Type	Proton Conductivity (S/cm)			Acid Doping*	Acid Leaching (%)
	140 ℃	165 ℃	180 ℃		
PBI	0.055	0.072	0.085	12.7	83.5
PBI/BN-2.5	0.230	0.250	0.260	12.9	70.9
PBI/BN-5.0	0.150	0.165	0.179	11.7	72.3
PBI/BN-7.5	0.075	0.086	0.092	10.8	76.7
PBI/BN-10	0.095	0.115	0.125	11.2	75.6

* The number of H_3PO_4 moles per PBI repeat unit

It was observed that the proton conductivity of all membranes spiked with elevating temperature, as shown in Table 4.4. Since temperature plays a key role in the kinetics of proton movements in the PBI and the movability of polymer chains, the conductivity of all membranes increased with temperature. This trend may be attributed to the Grotthus proton conduction mechanism as previously studied in the literature [107]. On the contrary, the lowest proton conductivity was determined for PBI/BN-7.5 as 0.092 S/cm with the highest acid leaching among composite membranes 76.7 %. It seems that proton conductivity increases with the reduced acid leaching and elevated acid doping levels.

In order to decide on the proton conductivity mechanism, the conductivity data was used to calculate the activation energies by means of the Arrhenius equation, as shown below in (12) [108]:

$$\ln(\sigma.T) = ln\sigma_0 \quad - \frac{E_a}{RT} \tag{12}$$

In this equation, σ is the proton conductivity of the membrane (S cm^{-1}), E_a is the pre-exponential factor (S cm^{-1}), Ea is the proton-conducting activation energy (J mol^{-1}), R is the universal gas constant (J mol^{-1} K^{-1}) and T is the absolute temperature (K).
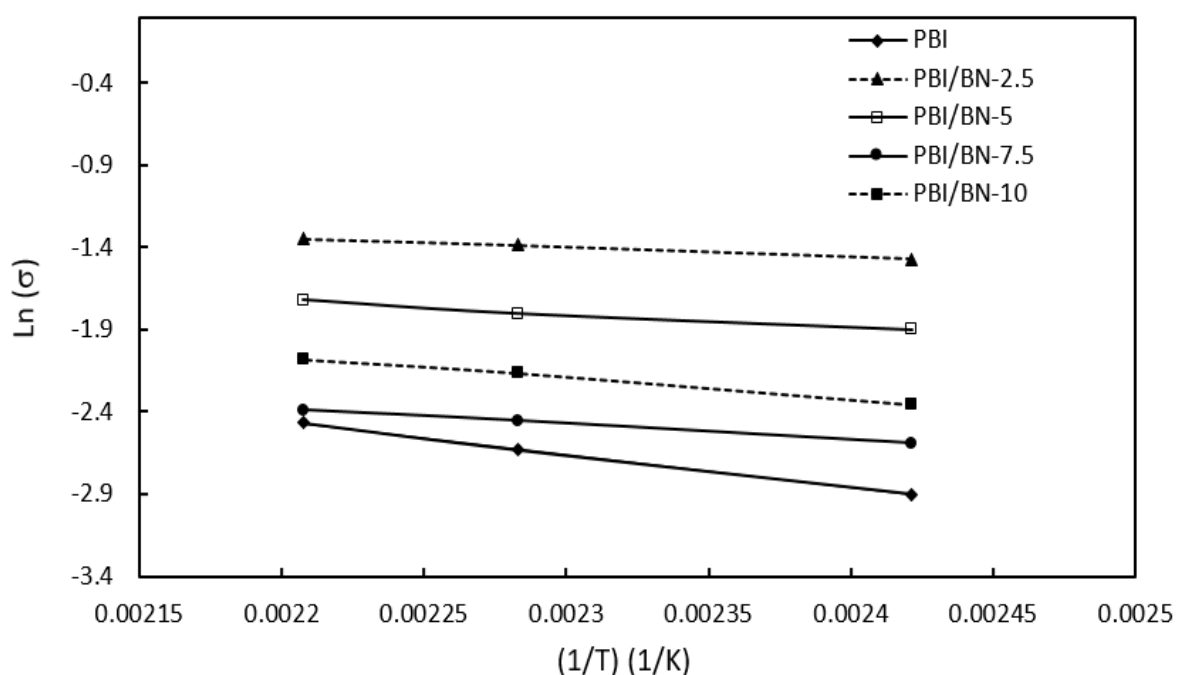

Figure 4.2 Arrhenius plots of PBI and PBI composite membranes.

The activation energy (Ea) of the membranes was calculated from the temperature-dependent conductivity of the proton from 140 ℃ to 180 ℃ under dry conditions by linear regression and using the Arrhenius equation. To decide on the ion transport activation energy and conduction model, the Arrhenius plots were drawn for each membrane, as in Figure 4.2 showing typical Arrhenius plots for the conductivity temperature relation according to Equation (12). The pure PBI activation energy was determined as 16.84 kJ/mol. The activation energy values of the membranes were determined using the slope of the plots. The temperature dependence of the proton's conductivity in polymer electrolytes considered as a specific type of the proton conductivity mechanism. The Ea values of PBI/BN-2.5, PBI/BN-5.0, PBI/BN-7.5 and PBI/BN-10 membranes are 4.80 kJ/mol, 6.78 kJ/mol, 7.88 kJ/mol, 7.88 kJ/mol and 10.77 kJ/mol respectively.

4.5   Mechanical Test Results

Determination of the mechanical stability of the PBI/BN composite membrane is one of the critical parameters in determining the HT-PEMFC performance of the membrane. Tensile test was performed to study the effect of different weights of BN as a filler on the mechanical properties of the PBI membrane. Adequate mechanical strength is essential for HT-PEMFC application to possess to withstand the fabrication of membrane electrode assemblies. The mechanical properties of the membranes are shown in Table 4.2.

Table 4.2 Mechanical test results of membranes.

Membrane	Tensile Strength (MPa)	Elongation at Break (%)
PBI	6.67	92.7
PBI/BN-2.5	7.46	106.3
PBI/BN-5	8.64	114.4
PBI/BN-7.5	8.75	131.8
PBI/BN-10	5.93	85.4

The tensile strength of the PBI, PBI/BN-2.5, PBI/BN-5.0, PBI/BN-7.5 and PBI/BN-10 membranes were obtained as 6.67 MPa, 7.47 MPa, 8.64 MPa, 8.75 MPa, and 5.93 MPa, respectively. The lowest tensile strength and elongation at break values were

determined for PBI/BN-10 composite membrane that can be attributed to the non-homogeneous dispersion of BN particles in the PBI polymer matrix as confirmed by SEM image membrane in Figure 4.2. The PBI/BN membranes can adequately get the requirement of HT-PEMFC.

4.6   SEM Results

The surface morphology of the composite membrane is of considerable significance. The most important challenge in composite membrane preparation with nanoparticles is the high agglomeration tendency due to the increased surface energy of the particles, thereby leading to low thermal and mechanical properties [109]. The compatibility of inorganic fillers and organic polymers has also important impacts on the membrane's mechanical, thermal and optical properties. For this reason, SEM analysis was performed to observe the morphology of the membranes. Figure 4.3 shows the cross-section SEM images of the PBI/BN composite membranes with ×20000 and ×50000 magnification. As seen from Figure 4.3 (a-d), the BN particles in the PBI/BN-2.5 and PBI/BN-5 membranes were homogenously distributed within the matrix. This can be explained by the good interaction of hydrogen bonding between the PBI matrix and BN. However, PBI/BN-7.5 and PBI/BN- 10 membranes showed some BN agglomerations in the polymer matrix.

Figure 4.4 illustrates the surface SEM analysis of PBI/BN-2.5 membrane. The EDX spectra of the PBI/BN-2.5 composite membrane is also displayed in Figure 4.4. The spectra indicate the presence of carbon (C), oxygen (O), Nitrogen (S) and Boron (B) confirming that the BN fillers incorporated in the PBI matrix were successfully attached to the polymer network. The bright dots with the colors of blue, red, green and yellow represent C, N, O and B, respectively. The mapping images confirm that all the elements demonstrated a uniform distribution in the PBI/BN-2.5 membrane surface.
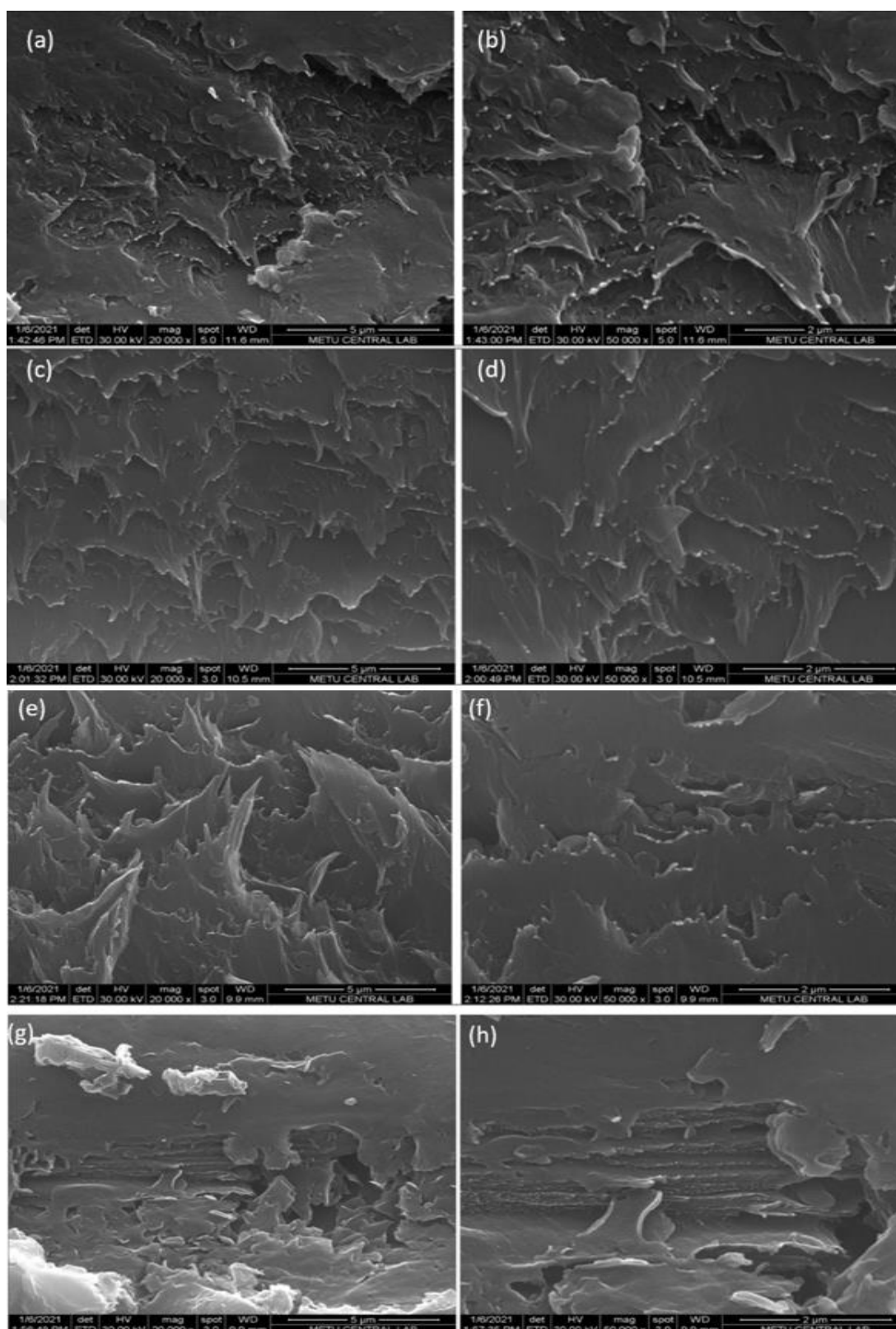
Figure 4.3 Cross Section SEM image of (a) × 20000, (b) ×50000 of PBI/BN-2.5, (c) ×20000 and (d) ×50000 of PBI/BN-5, (e) ×20000 and (f) ×50000 of PBI/BN-7.5, (g) ×20000 and (h) ×50000 of PBI/BN-10 membranes.
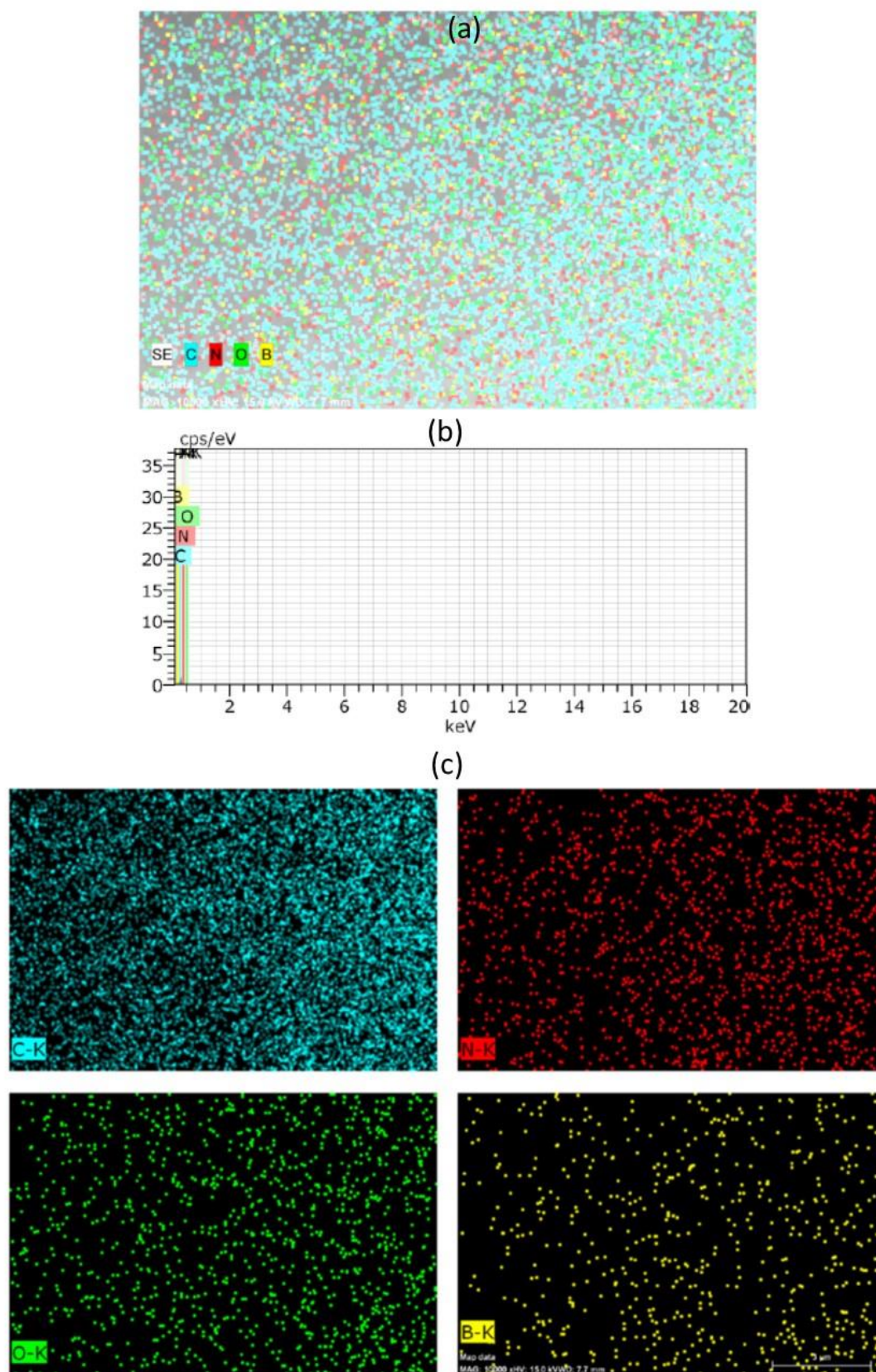
Figure 4.4 SEM analysis of a) Surface, b) EDX spectra and c) Mapping of PBI/BN-2.5 membrane (×10000).

4.7   HT-PEMFC Test

The PBI/BN-2.5 composite membrane was selected for HT-PEMFC performance studies due to its homogeneous BN distribution, highest proton conductivity, and better mechanical properties. The performance of the MEA based on PBI/BN-2.5 membrane was compared with that of the MEA based on the PBI. Figure 4.5 shows the HT-PEMFC performance comparison of the PBI membrane and PBI/BN-2.5 composite membrane at 165℃ with H_2 and dry Air.
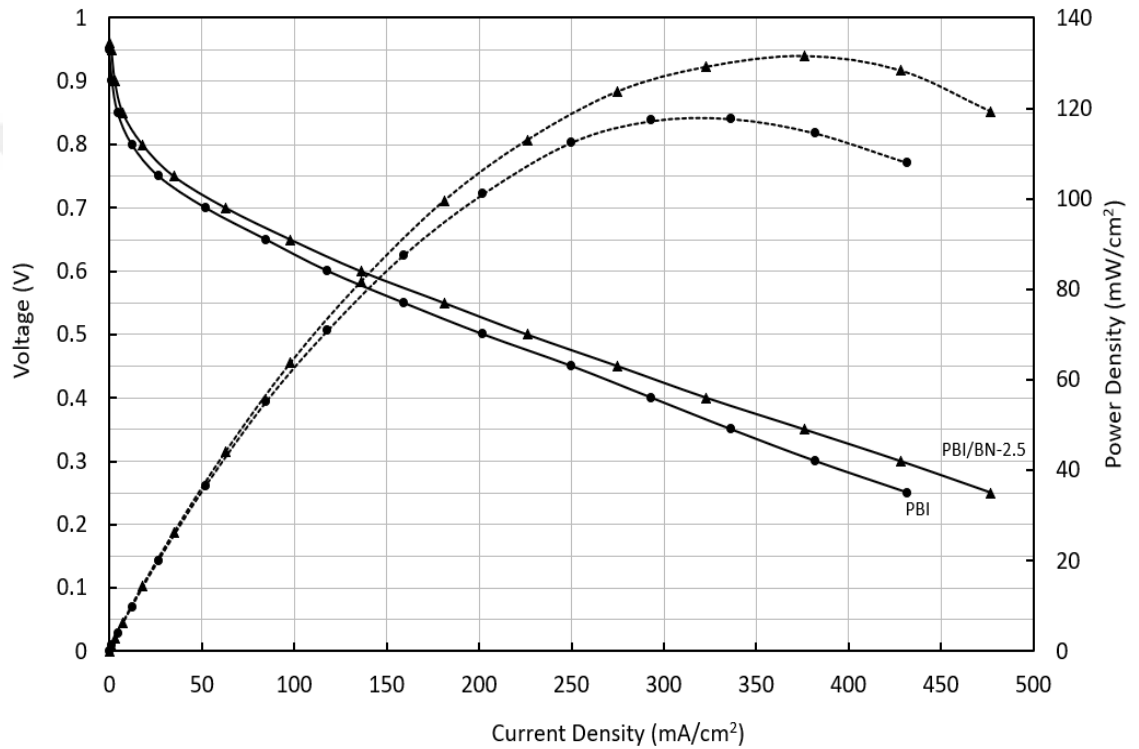
Figure 4.5 Comparison of PEMFC performance of PBI and PBI/BN-2.5 membranes at 165℃ with H_2 and Air.

The HT-PEMFC tests displayed an open circuit voltage (OCV) of approximately 0.97-0.94 V for the commercial PBI and PBI composite membrane. These are quite satisfactory values for both as high OCV values indicate that there was neither an H_2 crossover through the membrane, nor a pinhole formation in MEA [110]. The current density for PBI/BN-2.5 was found to be 136 mA/cm^2, and maximum power density was determined as 132 mW/cm^2. The commercial PBI membrane reached 118 mW/cm^2 maximum power density 0.118 and mA/cm^2. High performance of the PBI/BN-2.5-based MEA can be attributed to high proton conductivity within the

membrane. In addition, the low acid leaching of the PBI/BN-2.5 membrane is effective in achieving high HT-PEMFC performance. As a result, proton conductivity in the PBI/BN-2.5 membrane lasts longer compared to the PBI membrane
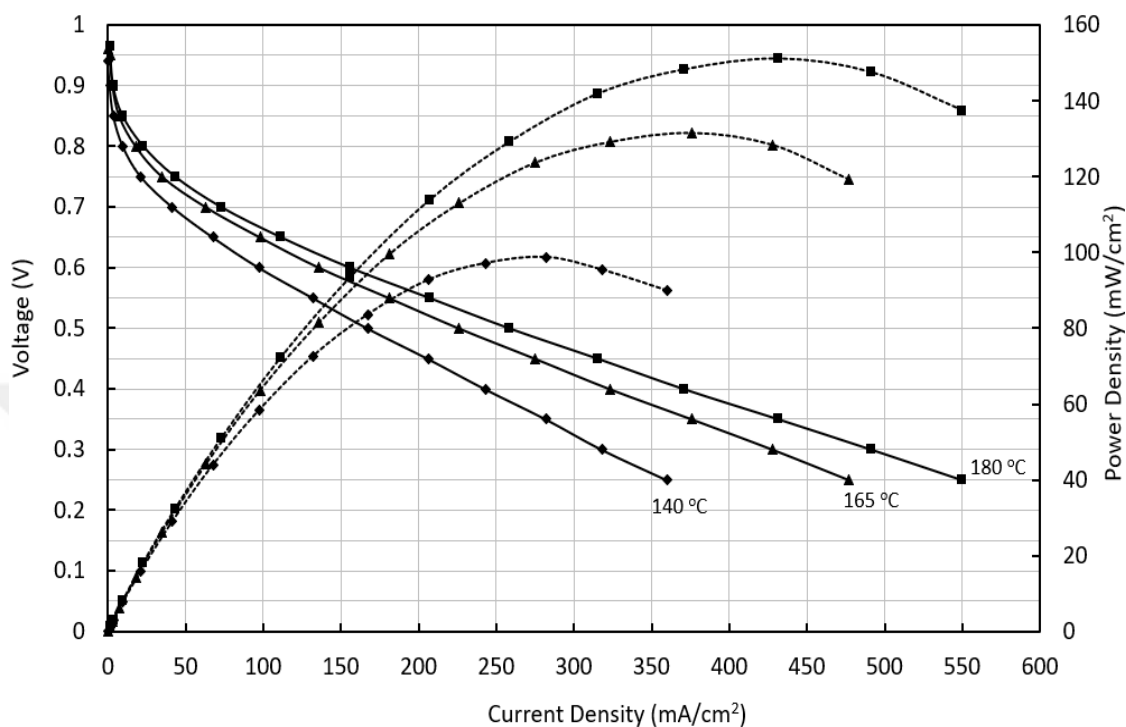
Figure 4.6 shows the effect of working temperatures on HT-PEMFC performance of the PBI/BN-2.5 composite membrane. The performance tests were evaluated at three different temperature (140 °C, 165 °C and 180 °C) with H_2 and Air.

Figure 4.6 illustrates the temperature effect on the PEMFC performance of PBI/BN-2.5 with H_2 and Air. The OCV values of the PBI/BN-2.5 membrane were determined as 0.94, 0.96 and 0.965 V for 140 °C, 165 °C and 180 °C, respectively. Again, the high performance of this MEA can be attributed to high proton conductivity of the membrane. The maximum power densities of the PBI/BN-2.5 membrane was obtained as 99, 132 and 151 mW/cm^2 for 140 °C, 165 °C and 180 °C, respectively. The HT-PEMFC performance was seen to increase with working temperature, and the lowest performance was determined at 140°C, ascribed to lower proton conductivity at 140°C. The obtained results show that the BN particles added to PBI matrix have a positive effect on the HT-PEMFC performance. Table 4.3 summarizes the HT-PEMFC results of the PBI/BN-2.5 and PBI membranes.

Table 4.3 HT-PEMFC test results of PBI/BN-2.5 and PBI membranes.

Membrane	Temperature (^{o}C)	OCV (V)	Current Density @0.6 V (mA/cm^2)	Max. Power Density (mW/cm^2)
PBI/BN-2.5	140	0.94	97.3	99
PBI/BN-2.5	165	0.96	136	132
PBI/BN-2.5	180	0.965	156	151
PBI	165	0.95	118.2	118

CHAPTER 5

CONCLUSIONS

The aim of this study was to develop PBI/BN composite membranes for HT-PEMFC. For this, the membranes were prepared with the solution casting method and using PBI as a base membrane. The BN additive ratio was set as 2.5, 5, 7.5 and 10 wt. %. The effect of the BN filler on the thermal, morphological and mechanical properties were examined using TGA, SEM, mechanical test, and acid doping/leaching measurements.

The results show that the all PBI/BN composite membranes are thermally stable at the HT-PEMFC operating temperature. The acid doping level of PBI/BN-2.5 reached 12.9, the highest of all membranes. Likewise, the maximum proton conductivity obtained for PBI/BN-2.5 membrane is 0.260 S/cm at 180 ℃. The results confirm that BN particles significantly contribute to proton conductivity which may be explained with the formation of hydrogen bonds between PBI, doped H_3PO_4 and BN. However, the PBI/BN-7.5 and PBI/BN-10 membranes show poor performance concerning ADL, acid leaching and proton conductivity. According to the SEM analyses, the more agglomeration of the BN particles was observed in the composite membrane with a high BN concentration. The non-homogenous morphology can potentially develop cracks and, henceforth negatively affect the membrane characteristics, especially in mechanical terms.

The PBI/BN-2.5 composite membrane demonstrates high performance during the HT-PEMFC performance tests. The maximum power density for PBI/BN-2.5 is found to be 99, 132 and 151 mW/cm^2 for 140 °C, 165 °C and 180 °C, respectively. This high performance of can be attributed to the increased proton conductivity of the membrane. The performance results were compatible with those available in the literature, again confirming that both ADL and acid retention capability have a considerable effect on fuel cell performance. In the same vein, the obtained results reveal that the BN filler has a notable effect on the thermal, mechanical and electrochemical

properties of the membranes. Overall, the findings imply that the PBI/BN composite membrane in this study is a satisfactory potential candidate for use in HT-PEMFC operations.

Recommendations for future studies

- Studies can be directed toward long-term tests for HT-PEMFC with PBI/BN-2.5 composite membranes.

- Different gas diffusion layer and electrode structures can be designed for PBI/BN composite membranes.

- It is recommended to investigate homogeneous BN distribution with different surfactants for PBI/BN-7.5 and PBI/BN-10 composite membranes, which have low properties.

- The agglomeration of the BN particles in PBI matrix can be investigated for homogeneous BN distribution.

REFERENCES

[1]   A. Midilli, M. Ay, I. Dincer, and M. A. Rosen, "On hydrogen and hydrogen energy strategies Ⅰ: current status and needs," *Renewable and sustainable energy reviews,* vol. 9, pp. 255–271, 2005.

[2]   M. Mustafa, "Design and manufacturing of a (PEMFC) proton exchange membrane fuel cell.", PhD. Thesis, Coventry University, 2009.

[3]   P. P. Edwards, V. L. Kuznetsov, and W. I. F. David, "Hydrogen energy," *Philos. Trans. R. Soc. A Math. Phys. Eng. Sci.*, vol. 365, no. 1853, pp. 1043–1056, 2007.

[4]   P. Grimes, "*Historical pathways forfuel cells. the new electric century*", Annual Battery Conference on Applications and Advances, 2000, pp. 41-45.

[5]   M. Sankir, "Proton exchange membrane fuel cell systems based on aromatic hydrocarbon and partially fluorinated disulfonated poly (arylene ether) copolymers" , PhD. Thesis,Virginia Tech, 2005.

[6]   VR. Stamenkovic, BS. Mun, M. Arenz, K JJ. Mayrhofer, CA. Lucas, G. Wang, PN. Ross, and NM. Markovic. "Trends in electrocatalysis on extended and nanoscale Pt-bimetallic alloy surfaces." *Nature materials*" vol. 6, no. 3 (2007): 241-247.

[7]   N. Giordano, E. Passalacqua, L. Pino, AS. Arico, V. Antonucci, M. Vivaldi, and K. Kinoshita, 1991. Analysis of platinum particle size and oxygen reduction in phosphoric acid. *Electrochimica Acta*, vol. 36, no.13, pp.1979-1984.

[8]   A. Vassiliev, High Temperature PEM Fuel Cells and Organic Fuels. Department of Energy Conversion and Storage, PhD. Thesis, Technical University of Denmark, 2014.

[9]   MF. Jamil, "Synthesis of platinum nanoparticles on graphene via electrophoretic deposition as catalyst for PEMFC.", PhD. Thesis, 2017.

[10]   S. Mekhilef, R. Saidur, and A. Safari, "Comparative study of different fuel cell technologies," *Renew. Sustain. Energy Rev.*, vol. 16, no. 1, pp. 981–989, 2012.

[11]   A. Benrabeh, F. Khoucha, O. Herizi, M. E. H. Benbouzid, and A. Kheloui, "FC/battery power management for electric vehicle based interleaved DC-DC boost converter topology," in *2013 15th European Conference on Power Electronics and Applications (EPE)*, 2013, pp. 1–9.

[12]   JWD. Ng, TR. Hellstern, J. Kibsgaard, AC. Hinckley, JD. Benck, and TF. Jaramillo, "Polymer electrolyte membrane electrolyzers utilizing non-precious Mo-based hydrogen evolution catalysts," *ChemSusChem*, 2015, vol. 8, no. 20, pp. 3512–3519.

[13]   AB. Stambouli and E. Traversa, "Solid oxide fuel cells (SOFCs): a review of an environmentally clean and efficient source of energy,". *Renewable and sustainable energy reviews*, , 2002. vol. 6, no.5, pp. 433–455.

[14]   J. Marcinkoski, JP. Kopasz, and TG. Benjamin, "Progress in the US DOE fuel cell subprogram efforts in polymer electrolyte fuel cells," *Int. J. Hydrogen Energy*, vol. 33, no. 14, pp. 3894–3902, 2008.

[15]   S. Yerramalla, A. Davari, A. Feliachi, and T. Biswas, "Modeling and simulation of the dynamic behavior of a polymer electrolyte membrane fuel cell," *J. Power Sources*, vol. 124, no. 1, pp. 104–113, 2003.

[16]   E. Mancusi, É. Fontana, AA. Ulson De Souza, and SMA. Guelli Ulson De Souza, "Numerical study of two-phase flow patterns in the gas channel of PEM fuel cells with tapered flow field design," *Int. J. Hydrogen Energy*, 2014.

[17]   MT. Gencoglu and Z. Ural, "Design of a PEM fuel cell system for residential application," *Int. J. Hydrogen Energy*, vol. 34, no. 12, pp. 5242–5248, 2009.

[18]   P. Lin, P. Zhou, and C. W. Wu, "A high efficient assembly technique for large PEMFC stacks Part I . Theory," vol. 194, pp. 381–390, 2009.

[19]   Y. Ozdemir, Cross-linked polybenzimidazole membranes for high temperature PEM fuel cells. Master degree thesis. Middle East Technical University,Turkey, 2018.

[20] F. Barbir. *PEM fuel cells: theory and practice*. 2nd ed. Burlington: Elsvier; 2005, pp-197-200.

[21] Y. Devrim, A. Albostan, and H. Devrim. "Experimental investigation of CO tolerance in high temperature PEM fuel cells." *International Journal of Hydrogen Energy* vol. 43, no. 40, pp. 18672-18681, 2018.

[22] S. Pehlivan-Davis, "Polymer Electrolyte Membrane (PEM) fuel cell seals durability."PhD. Thesis, Loughborough University, 2016.

[23] N. Ul Hassan, M. Kilic, E. Okumus, B. Tunaboylu, and A. Murat Soydan, "Experimental determination of optimal clamping torque for AB-PEM fuel cell," *J. Electrochem. Sci. Eng.*, vol. 6, no. 1, pp. 9–16, 2016.

[24] C. Song and J. Zhang, "*PEM fuel cell electrocatalysts and catalyst layers*," Fundam. Appl. Springer, New York, 2008, vol. 89.

[25] S. ENDALKACHEW, "In Partial Fulfillment of the Requirements for the Degree of Master of Science in Geo-information." 2018.

[26] A. Jayakumar, S. Singamneni, M. Ramos, and A. M. Al-jumaily, "Manufacturing the Gas Diffusion Layer for PEM Fuel Cell Using a Novel 3D Printing Technique and Critical Assessment of the Challenges Encountered,". *Matierials,* , 2017, vol. 10, no.7, pp. 1–9.

[27] S. Holdcroft, "Fuel cell catalyst layers: a polymer science perspective," *Chem. Mater.*, 2014, vol. 26, no. 1, pp. 381–393.

[28] S. J. Peighambardoust, S. Rowshanzamir, and M. Amjadi, "Review of the proton exchange membranes for fuel cell applications." *International journal of hydrogen energy*, vol. 35, no.17, pp. 9349-9384. 2010.

[29] Y. Bahramzadeh, and M. Shahinpoor, "*A Review of Ionic Polymeric Soft Actuators and Sensors,*" , Soft Robotic, 2014, vol. 1, no. 1, pp. 38–52.

[30] T. Sata, "*Ion exchange membranes preparation, characterization, modification and application*. The Royal Society of Chemistry," 2004.

[31]   Q. Li, R. He, R. W. Berg, H. A. Hjuler, and N. J. Bjerrum, "Water uptake and acid doping of polybenzimidazoles as electrolyte membranes for fuel cells," *Solid State Ionic,* , 2004, vol. 168, pp. 177–185.

[32]   M. Li, Z. Shao, and K. Scott, "composite membrane for proton-exchange membrane fuel cells operating at high temperature," *Journal of Power Sources*, vol. 183, no. 1, pp. 69–75, 2008.

[33]   B. Smitha, S. Sridhar, and A. A. Khan, "Solid polymer electrolyte membranes for fuel cell applications — a review," *Journal of membrane science*, vol. 259, no. 1-2 pp. 10–26, 2005.

[34]   S. J. Peighambardoust, S. Rowshanzamir, and M. Amjadi, Review of the proton exchange membranes for fuel cell applications Review of the proton exchange membranes for fuel cell applications, *International journal of hydrogen energy*, vol. 35, no. 17, pp. 9349-9384. 2010.

[35]   M. Rikukawa and K. Sanui, "Proton-conducting polymer electrolyte membranes based on hydrocarbon polymers," vol. 25, 2000.

[36]   S. Motupally, A. J. Becker, and J. W. Weidner, "Diffusion of water in Nafion 115 membranes," *J. Electrochem. Soc.*, vol. 147, no. 9, p. 3171, 2000.

[37]   T. Oshima, M. Yoshizawa-fujita, Y. Takeoka, and M. Rikukawa, "Use of a High-Performance Poly(p‑phenylene)-Based Aromatic Hydrocarbon Ionomer with Superacid Groups in Fuel Cells under Low Humidity Conditions," 2016.

[38]   W. Gorecki, C. Berthier, F. Defendini, and C. Poinsignon, "F. DEFENDINI, C. POINSIGNON and M.B. A R M A N D," vol. 30, pp. 969–974, 1988.

[39]   S. Petty-Weeks, J. J. Zupancic, and J. R. Swedo, "Proton conducting interpenetrating polymer networks," *Solid State Ionics*, vol. 31, no. 2, pp. 117–125, 1988.

[40]   J. R. Stevens, W. Wieczorek, D. Raducha, and K. R. Jeffrey, "Proton conducting gel/H3PO4 electrolytes," *Solid State Ionics*, vol. 97, no. 1–4, pp. 347–358, 1997.

[41] R. Tanaka, H. Yamamoto, A. Shono, K. Kubo, and M. Sakurai, "Proton conducting behavior in non-crosslinked and crosslinked polyethylenimine with excess phosphoric acid," *Electrochim. Acta*, 2000, vol. 45, no. 8–9, pp. 1385–1389.

[42] S. Simon, F. Zhou, V. Liso, S. L. Sahlin, J. R. Vang, S. Thomas, and S. K. Kær, "A comprehensive review of PBI-based high temperature PEM fuel cells A Comprehensive Review of PBI-based High Temperature PEM Fuel Cells," *International Journal of Hydrogen Energy*, vol. 41, no. 46, pp. 21310-21344. September, 2016.

[43] H. Steininger, M. Schuster, K. D. Kreuer, A. Kaltbeitzel, B. Bingöl, H. M. Wolfgang, S. Schauff, G. Brunklaus, J. Maier, and H. W. Spiess. "Intermediate temperature proton conductors for PEM fuel cells based on phosphonic acid as protogenic group: A progress report," *Physical Chemistry Chemical Physics*, 2007, vol. 9, no. 15, pp. 1764–1773.

[44] M. T. D. Jakobsen, J. O. Jensen, L. N. Cleemann, and Q. Li, *Durability issues and status of PBI-Based fuel cells*. Springer, Cham., 2016 , pp. 487-509.

[45] C. Xu, "Development of membranes for low and intermediate temperature polymer electrolyte membrane fuel cell." , PhD diss., Newcastle University, 2013.

[46] Q. Li, R. He, J. O. Jensen, and N. J. Bjerrum, "PBI- based polymer membranes for high temperature fuel cells–preparation, characterization and fuel cell demonstration. ", *Fuel cells*, 2004, vol. 4, no. 3, pp. 147-159.

[47] H. Vogel, and C. S. Marvel, "Polybenzimidazoles, new thermally stable polymers. ", *Journal of Polymer Science*, vol. 50, no. 154, 511-539, 1961.

[48] C. B. Shogbon, J. L. Brousseau, H. Zhang, B. C. Benicewicz, , and Y. A. Akpalu, "Determination of the molecular parameters and studies of the chain conformation of polybenzimidazole in DMAc/LiCl. ", *Macromolecules*, 2006, vol. 39, no. 26, pp. 9409-9418.

[49] J. A. Asensio, E. M. Sánchez, and P. Gómez-Romero, "Proton-conducting membranes based on benzimidazole polymers for high-temperature PEM fuel

cells. ", *Chemical Society Reviews*, 2010, vol, 39, no. 8, pp. 3210-3239.

[50]   J. Bae, I. Honma, M. Murata, T. Yamamoto, M. Rikukawa, and N. Ogata, "Properties of selected sulfonated polymers as proton-conducting electrolytes for polymer electrolyte fuel cells", *Solid State Ionics*, 2002 vol. 147, no. 1-2, pp. 189-194.

[51]   J. Rozière, D. J. Jones, M. Marrony, X. Glipa, and B. Mula, "On the doping of sulfonated polybenzimidazole with strong bases. ", *Solid State Ionics*, 2001, vol. 145, no. 1-4, pp. 61-68.

[52]   M. Kawahara, M. Rikukawa, K. Sanui, and N. Ogata, "Synthesis and proton conductivity of sulfopropylated poly (benzimidazole) films,", *Solid State Ionics*, 2000, vol. 137, pp. 1193–1196.

[53]   J. A. Asensio and S. Borro, "Proton-Conducting Polymers Based on Benzimidazoles and EXPERIMENTAL", *Journal of Polymer Science Part A: Polymer Chemistry*, vol. 40, no. 21, pp. 3703-3710, 2002.

[54]   S. Rosini, and E. Siebert, "Electrochemical sensors for detection of hydrogen in air: model of the non-Nernstian potentiometric response of platinum gas diffusion electrodes". *Electrochimica acta,* 2005, vol. 50, no. 14, pp. 2943-2953.

[55]   R. Bouchet, E. Siebert, and G. Vitter, "Polybenzimidazole-Based Hydrogen Sensors I . Mechanism of Response with an E-TEK Gas Diffusion Electrode", *Journal of the Electrochemical Society*, vol. 147, no. 8, pp. 3125–3130, 2000.

[56]   D. Rathod, Æ. M. Vijay, Æ. N. Islam, R. Kannan, and Æ. U. Kharul, "Design of an '" all solid-state "' supercapacitor based on phosphoric acid doped polybenzimidazole (PBI) electrolyte", *Journal of applied electrochemistry,* vol. 39, no. 7, pp. 1097–1103, 2009.

[57]   J. S. Wainright, J. T. Wang, D. Weng, R. F. Savinell, and M. Litt, "Acid-doped polybenzimidazoles: a new polymer electrolyte", *Journal of the electrochemical society*, vol. 142, no. 7, L121, 1995.

[58]   X. Glipa, B. Bonnet, B. Mula, D. J. Jones, J. Rozie, and Â. Mole,

"Investigation of the conduction properties of phosphoric and sulfuric acid doped polybenzimidazole,", *Journal of Materials Chemistry*, vol. 9, no. 12, pp. 3045–3049, 1999.

[59] M. Y. Jang and Y. Yamazaki, "Preparation , characterization and proton conductivity of membrane based on zirconium tricarboxybutylphosphonate and polybenzimidazole for fuel cells,", *Solid State Ionic*, 2004 , vol. 167, no. 1-2, pp. 107–112.

[60] E. Quartarone, A. Magistris, , P. Mustarelli, S. Grandi, A. Carollo, G. Z. Zukowska, and S. Bodoardo, "Pyridine- based PBI Composite Membranes for PEMFCs", *Fuel Cells*, 2009, vol. 9, no. 4, pp. 349-355.

[61] J. Kerres and V. Atanasov, "ScienceDirect membranes : Stability , conductivity and fuel cell performance," *Int. J. Hydrogen Energy*, vol. 40, no. 42, pp. 1–13, 2015.

[62] V. Kurdakova, E. Quartarone, P. Mustarelli, A. Magistris, E. Caponetti, and M. L. Saladino, "PBI-based composite membranes for polymer fuel cells," *J. Power Sources*, vol. 195, no. 23, pp. 7765–7769, 2010.

[63] S. Singha, R. Koyilapu, K. Dana, and T. Jana, "Polybenzimidazole-Clay Nanocomposite Membrane for PEM Fuel cell : Effect of Organomodifier Structure," *Polymer (Guildf).*, 2019, vol. 167, pp. 13-20.

[64] Y. Wang, Z. Shi, J. Fang, H. Xu, and J. Yin, "Graphene oxide / polybenzimidazole composites fabricated by a solvent-exchange method," *Carbon N. Y.*, 2010, vol. 49, no. 4, pp. 1199–1207.

[65] Y. Wang, Z. Shi, J. Fang, H. Xu, X. Ma, and J. Yin, "Direct exfoliation of graphene in methanesulfonic acid and facile synthesis of graphene / polybenzimidazole nanocomposites,", *Journal of Materials Chemistry*, vol. 21, no. 2, pp. 505–512, 2011.

[66] S. Chuang, S. L. Hsu, and Y. Liu, "Synthesis and properties of fluorine-containing polybenzimidazole / silica nanocomposite membranes for proton exchange membrane fuel cells,", *Journal of Membrane* Science, vol. 305, no.1-2, pp. 353–363, 2007.

[67] P. Staiti, M. Minutoli, and S. Hocevar, "Membranes based on phosphotungstic acid and polybenzimidazole for fuel cell application,", *Journal of Power Sources*, vol. 90, no. 2, pp. 231–235, 2000.

[68] R. He, Q. Li, G. Xiao, and N. J. Bjerrum, "Proton conductivity of phosphoric acid doped polybenzimidazole and its composites with inorganic proton conductors,", *Journal of Membrane Science*, vol. 226, no. 1-2, pp. 169–184, 2003.

[69] S. M. J. Zaidi, "Preparation and characterization of composite membranes using blends of SPEEK / PBI with boron phosphate,", *Electrochimica Acta*, , 2005 vol. 50, no. 24, pp. 4771–4777.

[70] Y. Özdemir, N. Üregen, and Y. Devrim, "Polybenzimidazole based nanocomposite membranes with enhanced proton conductivity for high temperature PEM fuel cells," *Int. J. Hydrogen Energy*, vol. 42, no. 4, pp. 2648–2657, 2017.

[71] Y. Devrim, H. Devrim and I. Eroglu "ScienceDirect Polybenzimidazole / SiO 2 hybrid membranes for high temperature proton exchange membrane fuel cells," , *International Journal of Hydrogen Energy*, vol. 41 no. 23, pp. 10044-10052, 2016

[72] J. Lobato, P. Ca, M. A. Rodrigo, D. Úbeda, and F. J. Pinar, "A novel titanium PBI-based composite membrane for high temperature PEMFCs", *Journal of Membrane Science*, vol. 369, pp. 105–111, 2011.

[73] N. Üregen, K. Pehlivanoğlu, Y. Özdemir, and Y. Devrim, "Development of polybenzimidazole/graphene oxide composite membranes for high temperature PEM fuel cells", *International Journal of Hydrogen Energy*, vol. 42, no. 4, 2636-2647, 2017.

[74] R. Kannan, H. N. Kagalwala, H. D. Chaudhari, U. K. Kharul, S. Kurungot, and V. K. Pillai, "Improved performance of phosphonated carbon nanotube – polybenzimidazole composite membranes in proton exchange membrane fuel cells," *Journal of Materials Chemistry*, vol. 21, no. 20, pp. 7223–7231, 2011.

[75] H. Lin, T. L. Yu, W. Chang, C. Cheng, C. Hu, and G. Jung, "Preparation of a low proton resistance PBI / PTFE composite membrane,", *Journal of power*

sources, vol. 164, no. 2, pp. 481–487, 2007.

[76] P. Muthuraja, S. Prakash, V. M. Shanmugam, S. Radhakrsihnan, and P. Manisankar, "ScienceDirect Novel perovskite structured calcium titanate-PBI composite membranes for high-temperature PEM fuel cells : Synthesis and characterizations," *Int. J. Hydrogen Energy*, vol. 43, no. 9, pp. 1–10, 2017.

[77] D. Plackett, A. Siu, Q. Li, C. Pan, J. O. Jensen, S. F. Nieslsen , and N. J. Bjerrum, "High-temperature proton exchange membranes based on polybenzimidazole and clay composites for fuel cells," *J. Memb. Sci.*, vol. 383, no. 1–2, pp. 78–87, 2011.

[78] M. Moradi, A. Moheb, M. Javanbakht, and K. Hooshyari, "Experimental study and modeling of proton conductivity of phosphoric acid doped PBI-Fe2TiO5 nanocomposite membranes for using in high temperature proton exchange membrane fuel cell (HT-PEMFC)," *Int. J. Hydrogen Energy*, vol. 41, no. 4, pp. 2896–2910, 2016.

[79] J. Kim, K. Kim, T. Ko, J. Han, and J. Lee, "ScienceDirect Polybenzimidazole composite membranes containing imidazole functionalized graphene oxide showing high proton conductivity and improved physicochemical properties," *Int. J. Hydrogen Energy*, 2020.

[80] J. M. Chem, C. Xu, X. Wu, X. Wang, M. Mamlouk, and K. Scott, "Composite membranes of polybenzimidazole and caesium-salts-of- heteropolyacids for intermediate temperature fuel cells," , *Journal of Materials Chemistry*, vol. 21, no. 16, pp. 6014–6019, 2011.

[81] M. N. Hasan, M. Nafiujjaman, and Y.-K. Lee, "2D Nanomaterials for Gene Delivery," in *Biomedical Applications of Graphene and 2D Nanomaterials*, Elsevier, 2019, pp. 87–104.

[82] D. Smith, "can be found under https://www. chemistryworld. com/opinion/no-sexuality-please-were-scientists/7197. article," *Chem. World*, 2014, vol. 1.

[83] S. Hu, "Proton transport through one-atom-thick crystals,", *Nature*, 2014, vol. 516, no. 7530, pp. 227-230.

[84] S. Hu, M. Lozada-Hidalog, F. C. Wang, A. Mishchenko, F. Schedin, R. R.

Nair, E.W. Hill, D. W. Boukhvalov, M. I. Katsnelson, R. A. W. Dryfe, I. V. Grigorieva, H. A. Wu, and A. K. Geim, "Proton transport through one-atom-thick crystals", *Nature*, 2014, vol. 516, no. 7530, pp. 227-230

[85]   N. Ooi, V. Rajan, J. Gottlieb, Y. Catherine, J.B. Adams Structural properties of hexagonal boron nitride", *Modell Simul Mater Sci En*g, 2006, vol. 14, no. 3, pp.515.

[86]   G. Lee, M. Park, J. Kim, J. Ik, and H. Gyu, "Enhanced thermal conductivity of polymer composites filled with hybrid filler, " *Applied science and manufacturing*, 2006, vol. 37, no. 5, pp. 727–734.

[87]   M.W. Smith, K.C. Jordan, C. Park, W. Kim, P.T. Lille- hei, R. Crook, and J. S. Harrison, "Very long single- and few-walled boron nitride nanotubes via the pressurized vapor/condenser method ", *Nanotechnology*, 2009, vol. 20, no. 50 pp. 505-604.

[88]   R.N. Muthu, S. Rajashabala, R. Kannan "Synthesis and characterization of polymer (sulfonated poly-ether-ether-ketone) based nanocomposite (h-Boron nitride) membrane for hydrogen storage", *Int J Hydrogen Energy*, vol. 40, no. 4, pp. 1836-1845, 2015.

[89]   D. Golberg, Y. Bando, Y. Huang, T. Terao, M. Mitome, C. Tang, et al. Boron nitride nanotubes and nanosheets ACS Nano, 4 (2010), pp. 2979-2993.

[90]   G. Pezzotti, I. Kamada, and S. Miki, "Thermal conductivity of AlN / polystyrene interpenetrating networks", *Journal of the European Ceramic Society*, vol. 20, no.8 , pp. 1197–1203, 2004.

[91]   K. Watanabe, T. Taniguchi, H. Kanda, "Direct-band gap properties and evidence for ultraviolet lasing of hexagonal boron nitride single crystal", *Nature Material*, 2004, vol.3, no.6, pp. 404-409.

[92]   W. Meng, Y. Huang, Y. Fu, Z. Wanga, C. Zhi, "Polymer composites of boron nitride nanotubes and nanosheets", *Journal of Materials Chemistry*, vol. 2, no. 47, pp. 10049-10061, 2014.

[93]   R.K. Nagarale, W. Shin, P.K. Singh, "Progress in ionic organic-inorganic composite membranes for fuel cell applications", *Polymer Chemistry*, 2010,

vol. 1, no. 4, pp. 388-408.

[94]   M. Akel, S.U. Celik, A. Bozkurt, A. Ata, "Nano hexagonal boron nitride–nafion composite membranes for proton exchange membrane fuel cells", *Polymer Composites*, 2014, vol. 37, no. 2, pp. 422-428.

[95]   H. Fang, S. Bai, and C. P. Wong, "Composites Communications," *Composites*, 2016, vol. 2, pp. 19–24.

[96]   P. Dibandjo, L. Bois, F. Chassagneux, D. Cornu, J.M. Letoffe, B. Toury, and P. Miele, "Synthesis of boron nitride with ordered mesostructure," *Advanced Materials*, 2005, vol. 17, no. 5, pp. 571-574.

[97]   X. Zhang, G. Lian, S.J. Zhang, D.L. Cui, Q.L. Wang, "Boron nitride nanocarpets: controllable synthesis and their adsorption performance to organic pollutants", *Cryst Eng Comm*, 2012, vol. 14, no. 14, pp. 4670-4676.

[98]   W. Lei, D. Portehault, D. Liu, S. Qin, Y. Chen ,"Porous boron nitride nanosheets for effective water cleaning", *Nature communications*, 2013, vol. 4, no. 1, p. 1-7.

[99]   D. Ergun, Y. Devrim, N. Bac, and I. Eroglu, "Phosphoric Acid Doped Polybenzimidazole Membrane for High Temperature PEM Fuel Cell," *Journal of applied polymer science*, vol. 124, no. S1, pp.E267-E277

[100]   ASTM D638 - Standard Test Method for Tensile Properties of Plastics n.d. http://benttram.com/Standard_ASTMD638.html (accessed November 6, 2017).

[101]   R. E. Rosli, A. B. Sulong, W. R. W. Daud, and M. A. Zulkifley, "High-Temperature Proton Exchange Membrane Fuel Cell (HT-PEMFC) system," *Int. J. Hydrogen Energy*, pp. 1–22, 2016.

[102]   S. Erkan, "Effects of membrane electrode assembly components on proton exchange membrane fuel cell performance," *International Journal of Hydrogen Energy*, vol. 33, no. 1, pp. 165–170, 2008.

[103]   L. B. Boinovich, A. M. Emelyanenko, A. S. Pashinin, C. H. Lee, J. Drelich, and Y. K. Yap, "Origins of Thermodynamically Stable Superhydrophobicity

of Boron Nitride Nanotubes Coatings," *Langmuir*, 2012, vol. 28, no. 2, pp. 1206-1216.

[104] H. Pu, W. H. Meyer, and G. Wegner, "Proton Transport in Polybenzimidazole Blended with H3PO4 or H2SO4," *Journal of Polymer Science Part B: Polymer Physics*, vol. 40, no. 7, pp. 663–669, 2002.

[105] Y.L. Ma, J. S. Wainright, M. H. Litt, and R. F. Savinell ,"Conductivity of PBI Membranes for High-Temperature Polymer Electrolyte Fuel Cells service Conductivity of PBI Membranes for High-Temperature Polymer Electrolyte Fuel Cells," *Journal of the Electrochemical Society*, vol. 151, no. 1, 2004.

[106] M. Kulkarni, R. Potrekar, R. A. Kulkarni, and S. P. Vernekar, "Synthesis and Characterization of Novel Polybenzimidazoles bearing Pendant Phenoxyamine Groups," *Journal of Polymer Science Part A: Polymer Chemistry*, vol. 46, no. 17, pp. 5776–5793, 2008.

[107] J. M. Chem, S. Ghosh, S. Maity, and T. Jana, "Polybenzimidazole / silica nanocomposites : Organic-inorganic hybrid membranes for PEM fuel cell," *Journal of Materials Chemistry*, vol. 21, no. 38, pp. 14897–14906, 2011.

[108] M. Akel, S. Ünügür Çelik, A. Bozkurt, and A. Ata, "Nano hexagonal boron nitride-Nafion composite membranes for proton exchange membrane fuel cells," *Polym. Compos.*, 2016, vol. 37, no. 2, pp. 422-428.

[109] S. A. Vilekar and R. Datta, "The effect of hydrogen crossover on open-circuit voltage in polymer electrolyte membrane fuel cells," *Journal of Power Sources*, vol. 195, no. 8, pp- 2241-2247, 2010.